이학박사학위논문

다채널전극 시스템과 광유전학을 이용한 전대상피질에서의 통증관련 연구

Studies on the role of anterior cingulate cortex in pain-related behaviors by using multi-electrode array system and optogenetics

2016년 8월

서울대학교 대학원

뇌인지과학과

강 석 재

ABSTRACT

Studies on the role of anterior cingulate cortex in pain-related behaviors by using multi-electrode array system and optogenetics

Sukjae Kang

Department of Brain and Cognitive Sciences

The Graduate School

Seoul National University

Neurons in the anterior cingulate cortex (ACC) are assumed to play important roles in the perception of nociceptive signals and the associated emotional responses. Several studies have investigated the role of ACC in various ways, but still many needs to be solved. Long-term depression (LTD), a key form of synaptic plasticity important in learning and information storage in the brain, has been studied in various cortical regions including the ACC but the specific characteristic of LTD in ACC was not studied intensely. Therefore, in the first part of the study, a multi-electrode array system was used to map cingulate LTD in a spatiotemporal manner within the ACC. We found that low-frequency stimulation (1 Hz, 15min) applied onto deep layer V induced LTD in layers II/III and layers V/VI. Cingulate LTD requires activation of metabotropic glutamate

receptors (mGluRs), while L-type voltage-gated calcium channels and NMDA receptors also contribute to its induction. Peripheral amputation of the distal tail impaired ACC LTD, an effect that persisted for at least two weeks. The loss of LTD was rescued by priming ACC slices with activation of mGluR1 receptors by co-applying DHPG and MPEP, a form of metaplasticity that involved the activation of protein kinase C. These results provide *in vitro* evidence on the spatiotemporal properties of ACC LTD in adult mice. We demonstrate that tail amputation causes LTD impairment within the ACC circuit and that this can be rescued by activation of mGluR1.

In the second study, we focused on the fact that the neuronal types within the ACC that mediate these functions are poorly understood. Thus, optogenetic techniques was used to selectively modulate excitatory pyramidal neurons and inhibitory interneurons in the ACC and to assess their ability to modulate peripheral mechanical hypersensitivity in freely moving mice. We found that selective activation of pyramidal neurons rapidly and acutely reduced nociceptive thresholds and that this effect was occluded in animals made hypersensitive using Freund's Complete Adjuvant (CFA). Conversely, inhibition of ACC pyramidal neurons rapidly and acutely reduced hypersensitivity induced by CFA treatment. A similar analgesic effect was induced by activation of parvalbumin (PV) expressing interneurons, whereas activation of somatostatin (SOM) expressing interneurons had no effect on pain thresholds. These results provide direct evidence of the pivotal role of ACC excitatory neurons, and their regulation by PV expressing interneurons, in nociception.

Keywords : ACC, pain, LTD, optogenetics

Student Number : 2010-22724

CONTENTS

LIST OF FIGURES

CHAPTER I

INTRODUCTION

BACKGROUND

Physiological pain or acute pain is a critical protective function for animals and humans, whereas pathological pain or chronic pain causes major suffering among patients. Investigations of cellular mechanisms for physiological and pathological pain are focused mainly on the periphery and the spinal dorsal horn, considering potential less central side effects of drugs. However, despite progress achieved over many years, many forms of chronic pain are still resistant to conventional analgesics and drugs. Cumulative evidence consistently suggests that forebrain neurons including neurons in the anterior cingulate cortex (ACC) and insular cortex are important for pain-related perception. ACC is a highly wired cortical region around the rostrum of the corpus callosum. Neurons in the ACC receive inputs directly or indirectly from other regions of brain, including the thalamus, amygdala, hippocampus, and other cortical regions (Koechlin et al., 2003; Likhtik et al., 2005; Vogt, 2005; Wang and Shyu, 2004; Wei et al., 1999; Zhuo, 2008). Different functions of the ACC subregions have been proposed, mostly from human imaging studies (Bush et al., 2000). However, it remains to be determined at synaptic and molecular levels whether such function-specific regions indeed exist within the ACC. Studies from both human and animals consistently suggest that the ACC and its related areas are important for processing of pain perception. Lesions of the medial frontal cortex, including the ACC, significantly increased acute nociceptive responses as well as injury related aversive memory behaviors (Johansen et al., 2001; Lee et al., 1999).

Electrophysiological recordings from both animals and humans demonstrate that neurons within the ACC respond to noxious stimuli and are activated during pain anticipation or pain avoidance behavior (Hutchison et al., 1999; Koyama et al., 2000; Koyama et al., 1998; Kuo and Yen, 2005; Sikes and Vogt, 1992; Yamamura et al., 1996). Neuroimaging studies further confirm these observations and show that the ACC, together with other cortical structures, is activated by acute noxious stimuli, psychological pain, and social pain (Casey, 1999; Eisenberger et al., 2003; Iwata et al., 2005; Rainville et al., 2001; Rainville et al., 1997; Singer et al., 2004; Talbot et al., 1991; Wu et al., 2005c). Thus, understanding of synaptic mechanisms within the ACC will greatly help us to gain insights into plastic changes in the brain related to central pain.

Glutamate mediates excitatory transmission

Glutamate is the major fast excitatory transmitter in the ACC. Bath application of 6-cyano-7-nitroquinoxaline-2,3-dione (CNQX) completely abolishes fast excitatory postsynaptic currents (EPSCs) recorded in ACC neurons (Wu et al., 2005b). In addition to the a-amino-3-hydroxy-5-methyl-4-isoxazolepropionic acid (AMPA) receptor, postsynaptic glutamate kainate (KA) receptors contribute to fast excitatory synaptic transmission in the ACC. Single focal stimulation could induce small KA receptor-mediated EPSCs in the presence of a selective AMPA receptor antagonist, GYKI 53655.

GABA mediates inhibitory transmission

g-Aminobutyric acid (GABA) is the major inhibitory transmitter in the ACC. The inhibitory postsynaptic currents (IPSCs) are mainly mediated by postsynaptic $GABA_A$ receptors. Bath application of picrotoxin completely abolishes spontaneous IPSCs and evoked IPSCs (Wu et al., 2007). $GABA_B$ receptors are also found in ACC neurons, although the role of $GABA_B$ remains to be investigated. There are few studies that investigate the modulation of inhibitory transmission in the ACC. A recent study using KA knockout mice reported that inhibitory transmission in the ACC is under tonic modulation of KA GluR5 receptor (Zhao et al., 2005).

Long-term potentiation in ACC

Genetic, pharmacological and electrophysiological approaches have been used to investigate the basic mechanisms for long term potentiation (LTP) in ACC synapses. Different stimulation protocols can be used for inducing LTP in ACC pyramidal cells. Pairing training protocol (synaptic activity paired with postsynaptic depolarization), the spike-excitatory postsynaptic potential (EPSP) pairing protocol, and theta burst stimulation (TBS) protocol all induce LTP in ACC pyramidal neurons . Unlike the field recordings induced by TBS, LTP induced by the pairing protocol in intracellular recording, is mainly triggered by the activation of N-methyl-D-aspartate (NMDA) receptors but not L-type voltage-gated calcium channels (L-VGCCs). In ACC pyramidal cells, NMDA receptor containing

NR2A or NR2B subunits contributed to most of the NMDA receptor currents. Bath application of NR2A antagonist NVP-AAM077 and NR2B antagonist ifenprodil/Ro compounds almost completely blocked NMDA receptor-mediated EPSCs as well as LTP. By contrast, the NR2A or NR2B antagonist alone only reduced LTP. Activation of NMDA receptors leads to an increase in postsynaptic Ca^{2+} in dendritic spines. Ca^{2+} serves as an important intracellular signal for triggering a series of biochemical events that contribute to the expression of LTP. Ca^{2+} binds to calmodulin (CaM) and leads to activation of calcium-stimulated signaling pathways. Postsynaptic injection of BAPTA completely blocked the induction of LTP, indicating the importance of elevated postsynaptic Ca^{2+} concentrations (Zhao et al., 2005). GluR1 subunit C-termical peptide analog Pep1-TGL blocked the induction of LTP, thus GluR1-PDZ interaction is also important in this process (Hayashi et al., 2000; Toyoda et al., 2007b). In the maintanence phase of LTP, PKMzeta blocker, ZIP, reduced the potentiation level of ACC LTP (Li et al., 2010).

Long-term depression in ACC

NMDA receptor-dependent and –independent long-term depression (LTD) are the two well know forms of LTD in synapses of the neuron (Collingridge et al., 2010). ACC LTD induced by presynaptic stimulation with postsynaptic depolarization is NMDA receptor dependent (Wu et al., 2005a; Zhao et al., 2005). However, NMDA receptor-independent LTD has been reported using field

potential recordings from adult ACC slices (Zhuo, 2005). Thus, different induction protocols result in different forms of ACC LTD. Unlike ACC LTP, inhibition of NR2A or NR2B is sufficient to block ACC LTD. Furthermore, in the presence of NR2B receptor blockade, strong LTD pairing protocol can rescue LTD. This finding suggests that postsynaptic Ca^{2+} signaling is critical for the induction of LTD. Paired-pulse facilitation (PPF) is not changed during LTD in the ACC, further supporting the idea that induction of LTD might depend on postsynaptic mechanisms. Consistently, ACC LTD was abolished in GluR2 knockout mice (Toyoda et al., 2007a; Toyoda et al., 2005).

Alteration of ACC plasticity after injury

One important question related to ACC plasticity is whether injury causes prolonged or long-term changes in synaptic transmission in the ACC of rodents. In vivo recording in the ACC of anesthetized rats was performed and when peripheral electric shocks strong enough to activate Aδ and C fibers, evoked field EPSPs. This sensory response was enhanced when the contralateral hind paw digit was amputated. The potentiation was long lasting, remaining enhanced for at least 120 min. In order to address whether synaptic changes may occur locally within the ACC, field EPSPs to focal ACC electrical stimulation was measured. Consistently, a long-lasting potentiation of field EPSPs after amputation lasted for at least 120 min. To test whether this potentiation requires persistent activity from the injured hind paw, a local anesthetic, QX-314, was injected into the hind

paw at 120 min after amputation. However, QX-314 injection did not significantly affect the synaptic potentiation induced by amputation (Wei and Zhuo, 2001).

Intracellular recordings from cingulate neurons of anesthetized rats were performed to find the reason of potentiation after amputation. There was a long-lasting membrane potential depolarization in ACC neurons of adult rats after digit amputation in vivo (Wu et al., 2005c). Shortly after digit amputation of the hind paw, the membrane potential of intracellularly recorded ACC neurons quickly depolarized and then slowly repolarized. The duration of this amputation induced depolarization was about 40 min. Anatomic staining revealed that these neurons were pyramidal neurons in the ACC. An NMDA receptor antagonist, MK-801, significantly reduced the depolarization. These results provide direct in vivo electrophysiological evidence that ACC pyramidal cells undergo rapid and prolonged depolarization after digit amputation, and this might be associated with the synaptic mechanisms for phantom pain. In ACC slices of rats with digit amputation, the same repetitive stimulation produced less or no LTD. The loss of LTD is regionally selective, and no change was found in other cortical areas (Wei et al., 1999)

Optogenetics

Optogenetics is a widely used technique combining optics and genetics to modulate activities of specific cells or regions. It has been a powerful tool since it was developed nearly a decade ago, and numerous studies have been published

using it. The beauty of this technique is the temporal and spatial resolution of light stimulation and the observation of direct responses by light. Specific neuron types of specific brain regions can be selected and light could be given any time point to discover its functional role. Moreover, optogenetics can be used to study the circuit of specific behavior (Tye and Deisseroth, 2012; Yizhar et al., 2011). With these advantages, many ambiguous theories have been elucidated more clearly and numerous new discoveries have been found. The technology is still developing and more exciting discoveries can be observed with it.

PURPOSE OF THIS STUDY

I was interested in the function of ACC in pain related behaviors. Several studies with intracellular recordings, discovered its molecular mechanisms in the synaptic level but not much is known about the spatial information of mice ACC in pain related situations. In this thesis I address this question at the synaptic level using MED64, a multielectrode array. With this device, I could record several extracellular field responses in the mice ACC simultaneously and observe any possible differences in different spatial area in the ACC. I also studied about the functional role of specific types of neurons in the ACC using optogenetics.

In chapter II, I use MED64 to discover the characteristics of ACC LTD in normal and tail-amputated mice. Pharmacological screening was performed in 1Hz low frequency stimulation (LFS) induced ACC LTD of normal mice. Then show that ACC LTD was impaired in tail-amputated mice and found a way to recover LTD.

In Chapter III, I use optogenetics to test whether pain related behaviors could be changed by modulating activities of specific neurons in ACC. Several cre-line mice were used to target specific neuron types, and detected the mechanical threshold of mice in chronic inflammation pain models with light on and off. I show the bidirectional modulation of hyperalgesia with these strategies, and observe the importance of ACC activity in pain-related situations.

CHAPTER II

Plasticity of metabotropic glutamate receptor dependent long-term depression in the ACC after amputation

INTRODUCTION

Human and animal studies consistently demonstrate that neurons in the anterior cingulate cortex (ACC) play important roles in pain perception and chronic pain conditions (see Vogt, 2005; Zhuo, 2008 for reviews). Brain imaging studies demonstrate that ACC and its related cortical areas, are activated by acute nociceptive stimuli (Craig et al., 1996; Dunckley et al., 2005; Rainville et al., 1997; Strigo et al., 2003; Talbot et al., 1991). ACC can be also activated during the empathy of pain, social rejection and other psychological pain conditions (de Tommaso et al., 2005; Eisenberger et al., 2003; Singer et al., 2004). ACC has been reported to be activated in different chronic pain conditions (Apkarian et al., 2005; Zhuo, 2008, 2011). Inactivation of the ACC, by surgical lesions or cell death caused by stroke, leads to the reduction of the unpleasantness of pain or reduced pain intensity (Pillay and Hassenbusch, 1992; Wong et al., 1997; Yen et al., 2005, 2009). Electrophysiological recording from human shows that many ACC neurons are indeed nociceptive (Hutchison et al., 1999). Animal studies of the ACC not only confirm the importance of ACC in nociception (Vogt, 2005; Zhuo, 2008, 2011), but also reveal molecular mechanisms for chronic pain (Zhuo, 2006, 2008). While peripheral injury triggers activity-dependent immediate early genes (Zhuo, 2006, 2011) and induces long-term potentiation (LTP) of excitatory synaptic responses in the ACC neurons (Wei and Zhuo, 2001; Xu et al., 2008), inhibition or genetic deletion of key molecules that are required for triggering LTP produces analgesic effects in animal models of chronic pain (Wang et al., 2011; Wei et al., 2002; Wu et al., 2005a). Recently, PKMzeta (PKMζ) has been

identified as a key enzyme required to maintain such injury-related LTP (Li et al., 2010).

In addition to LTP, long-term depression (LTD) has been also implicated in various brain functions (see Bliss and Cooke, 2011 for review). Two major types of LTD have been discovered: NMDA receptor-dependent and NMDA receptor-independent LTD (or metabotropic glutamate receptor-dependent LTD, mGluR-LTD). These two different forms of LTD are triggered by different induction protocols, and underlie different physiological/pathological functions (Collingridge et al., 2010), such as learning and memory (Manahan-Vaughan and Braunewell, 1999), behavioral flexibility (Kim et al., 2011; Nicholls et al., 2008), fragile X syndrome (Dolen et al., 2007), and drug addiction (Brebner et al., 2005). LTD has also been described in the ACC (Toyoda et al., 2005, 2007). In adult rats with single digit amputation, ACC LTD was impaired (Wei et al., 1999).

In the present study, we used a 64-channel multi-electrode dish (MED64) system, a two-dimensional electric activity monitoring device, to characterize LTD in adult mouse ACC. The MED64 system allows us to detect the field excitatory postsynaptic potentials (fEPSP) at multiple sites in mouse ACC, which is difficult to achieve with conventional field recording systems. We found that low-frequency stimulation induced mGluR-dependent LTD at the network level, and suggest the possible utility of targeting the mGluR1 for future treatment of patients with amputation-related pain.

EXPERIMENTAL PROCEDURES

Animals

Adult (8-12 week old) male C57BL/6 mice (Orient Bio. Inc., Korea) were used. All animals were housed under a 12 h light/dark cycle with food and water provided *ad libitum*. All works were conducted according to the policy and regulation for the care and use of laboratory animals approved by Institutional Animal Care and Use Committee in Seoul National University.

Amputation surgical procedure

C57BL/6 mice were gently anesthetized with isoflurane. Then 2.5 cm length of the tail was removed (Fig. 7A). Locktight instant glue was used to stop bleeding. For sham surgery mice, only the anesthesia procedure was carried out. Two weeks later, all mice were sacrificed for the preparation of brain slices.

Brain slice preparation

Adult male mice were anesthetized with isoflorane and the brains were removed and transferred to ice-cold artificial cerebrospinal fluid (ACSF) containing (in mM) 124 NaCl, 2.5 KCl, 2 $CaCl_2$, 2 $MgSO_4$, 25 $NaHCO_3$, 1 NaH_2PO_4, 10 glucose (pH 7.4). This ACSF was used throughout the experiment. Three coronal brain slices (300 μm), after the corpus callosum meets and contains ACC, were cut using a vibratome (Leica VT 1000S, Germany). The slices were placed in a submerged recovery chamber with oxygenated (95% O_2, 5% CO_2) ACSF at 26 °C for at least 2 h.

Preparation of the multi-electrode array

The multi-electrode array (MEA) system used in the current study was MED64 (Panasonic, Japan). The procedures for preparation of the MED64 system were similar to those of Oka et al. (1999). The MED64 probe (MED-P515A, 8 x 8 array, interpolar distance 150 μm, Panasonic) was superfused with ACSF at 28-30 °C, and maintained at a 2-3 ml/min flow rate. One planar microelectrode with monopolar constant current pulses (5-18 μA, 0.2 ms) was used for stimulation of the ACC slice. The stimulation site was selected within the deep layer V region. Before use, the surface of the MED64 probe was treated with 0.1% polyethyleneimine (Sigma, St. Louis, MO) in 25 mmol/L borate buffer (pH 8.4) overnight at room temperature.

Field potential recording in adult ACC slices

After 2 h recovery, one ACC slice was placed in a MED64 probe in a way most of the 64 electrodes located within the ACC. The slice was allowed to recover for 1 h after transfer. Electrical stimulation was delivered to one channel located within the deep layer V of the ACC, and evoked fEPSPs were monitored and recorded from the other 63 channels. The intensity of the stimuli was approximately 60-70 % of the intensity that induced the maximal number of responding channels determined by the input-output curve. Baseline responses were evoked at 0.017 Hz for at least 30 min before 1 Hz stimulation was given for 15 min to induce LTD (total 900 pulses). All other low-frequency stimulation (3 Hz, 5 Hz and 10 Hz) protocols also gave total 900 pulses. In most experiments,

4-5 channels near the stimulation site were selected for data analysis due to its reliable LTD induction probability. The averaged value of those channels was counted as one sample. All of the data were averaged every 4 min except (RS)-3,5-Dihydroxyphenylglycine (DHPG) applying experiments which were averaged every 2 min.

Drugs

Drugs were prepared as stock solutions for frozen aliquots at -20°C. 6-Cyano-7-nitroquinoxaline-2,3-dione (CNQX, 20 μM), nimodipine (10 μM), D(-)-2-amino-5-phosphonopentanoic acid (AP5, 50 μM), (+)-α-methyl-4-carboxylphenlyglycine (MCPG) (500 μM), DHPG (20 or 100 μM), 2-Methyl-6-(phenylethynyl)pyridine hydrochloride (MPEP, 10 μM), and (S)-(+)-α-Amino-4-carboxy-2-methylbenzeneacetic acid (LY367385, 100 μM), chelerythrine chloride (3 μM), KN 62 (10 μM), and KT 5720 (1 μM) were used in the current study. Drugs used in Fig. 6 were applied throughout the entire experiment. Others were infused during the period of the horizontal bar on the graphs. AP5, nimodipine, MCPG, CNQX, chelerythrine chloride, KN 62, KT 5720 were purchased from Tocris Bioscience (Bristol, UK), and DHPG, MPEP and LY367385 from Abcam Biochemicals (Cambridge, UK).

Data analysis

MED64 Mobius was used for data acquisition and analysis. All data are presented as mean ± SEM. The percentages of the fEPSP slopes were normalized by the averaged value of the baseline (15-30 min). The depression levels used in

histograms are the averaged fEPSP slope value of the last 10 min of the experiment. We defined LTD in a channel if the response was depressed by at least 15% of baseline, during this period. Statistical comparisons were made using the t-test, one-way ANOVA, and Pearson product moment correlation test by SigmaPlot 11.0. Post hoc Bonferroni test was used for further comparison. If the data did not pass the equal variance test, one way ANOVA was done in ranks and Dunn's method was used for post-hoc test. In all cases, statistical significance was indicated by * $p < 0.05$, ** $p < 0.01$, *** $p < 0.001$.

RESULTS

Spatial distribution of extracellular responses in the ACC

In the present study, a 64 channel multi-electrode array, MED64, was used to record the spatial distribution of extracellular field responses in the ACC of adult mice. An ACC slice was placed on top of the 8 x 8 square shaped MED64 probe electrodes (Fig. 1A). One channel that covered the deep layer V of ACC was chosen to stimulate the slice (yellow circle in Fig. 1B). fEPSPs recorded from the remaining 63 channels were intensity dependent. This could be seen in single channel (Channel 29) and throughout the remaining channels (Fig. 1C, D and E). Most reliable fEPSPs were observed at recording sites located within the 450 μm range from the stimulation site. The amount of channels that show fEPSPs is also dependent on the intensity of the stimulation. In 3 mice (6 slices), we counted the number of channels generating a detectable fEPSP response over a stimulus intensity range varying from 5 to 18 μA. We found that the number of responsive channels reached a maximum at 12 μA with approximately 63% (on average 40 channels out of 63) generating a detectable response (Fig. 1F). The effective intensity to induce 50% of the maximum number of channels (32%) was 7.4 μA. In further experiments we set the stimulus intensity (typically 8 or 9 μA) to achieve a baseline response that was approximately 60-70 % of the maximum.

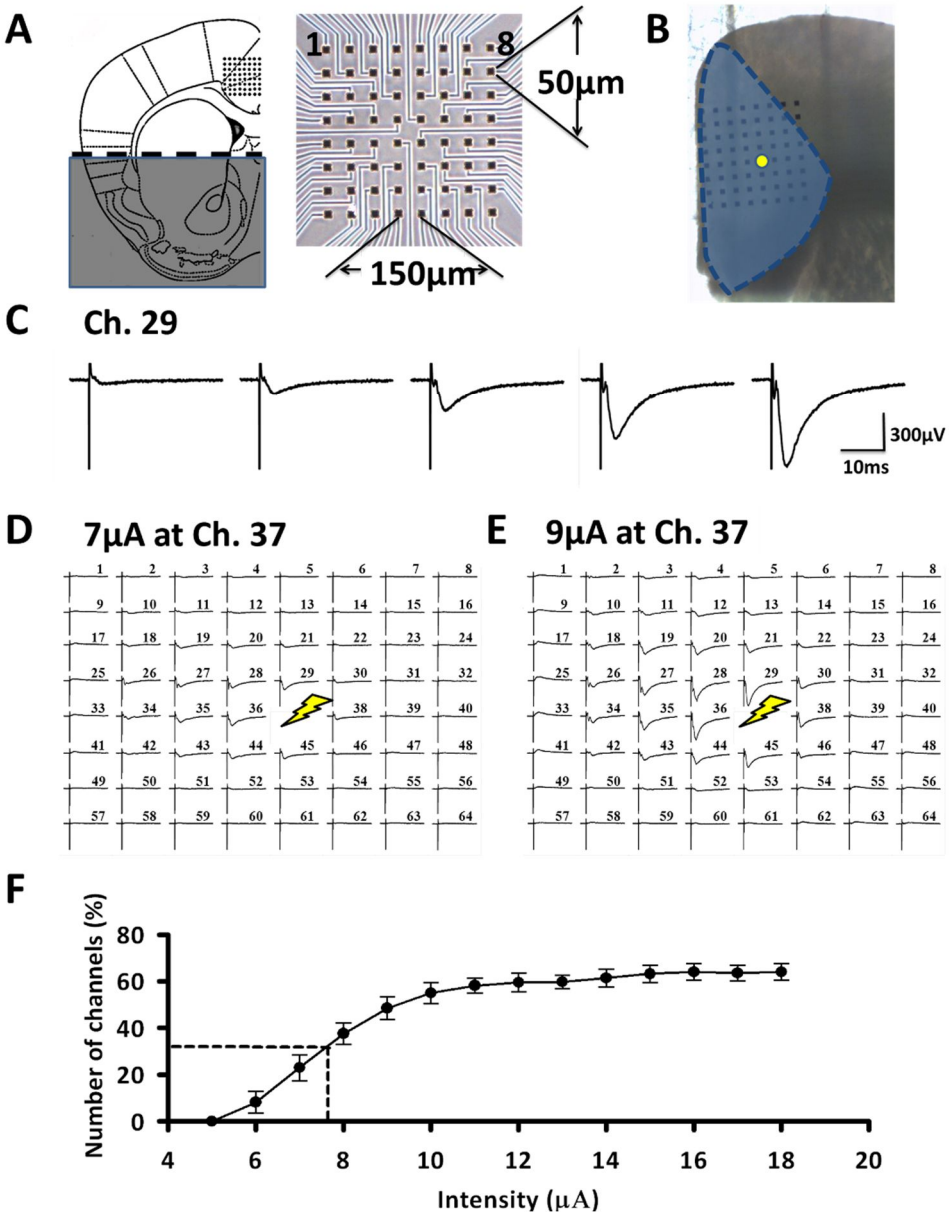
A
1
8
50μm
150μm
B
C
Ch. 29
300μV
10ms
D
7μA at Ch. 37
E
9μA at Ch. 37
F
Number of channels (%)
Intensity (μA)

Figure 1. Spatial distribution of excitatory synaptic transmission in the ACC on a multi-electrode array

A, Schematic diagram of an ACC slice placement on the MED64 probe, and the scale of the electrodes. The dark region in the slice is removed before recording.

B, Light microscopy photograph showing ACC and the MED64 probe electrodes. The blue colored region is the ACC and the yellow circle is the electrode (Channel 37) that is stimulated. Example traces on the graph indicate the responses in the numbered period.

C, Intensity dependent fEPSPs (5-9 μA) in one specific channel above the stimulation site (Channel 29).

D, E, All channel fEPSPs when stimulating channel 37 (yellow thunderbolt) with 7 μA and 9 μA. The number of channels exhibiting a response and the amplitude of the fEPSPs increased with raised stimulus intensities. The spreading of the fEPSPs displays the network in the ACC.

F, The number of activated channels increased as the input intensity was raised (n = 6 slices/ 3 mice). The effective intensity to induce 50% of the maximum (dashed line) was 7.4 μA. The number of activated channels became saturated around 12 μA.

Glutamate-mediated synaptic transmission in the ACC

Previous electrophysiological experiments have demonstrated that postsynaptic transmission in layer II/III of adult ACC is mediated by glutamatergic AMPA and kainate receptors in both rats and mice (Wei et al., 1999; Wu et al., 2005b). To confirm the pharmacological nature of fEPSPs, bath application of CNQX (20 μM, 20 min), an AMPA/kainate receptor antagonist that effectively blocks fast synaptic transmission (Blake et al., 1988), was used to determine whether these receptors were the major mediators of excitatory synaptic transmissions in all layers of ACC. After bath applying CNQX, all the fEPSPs in the ACC were blocked (Fig. 2A), indicating that fEPSPs recorded in every layer of ACC are mediated by glutamate acting on AMPA/kainate receptors. The time course of the effect of CNQX in a single channel example (Ch. 29; Fig. 2B), the averaged fEPSPs of all activated 20 channels in a single slice (Fig. 2C) and the average of three mice (n = 3 slices/ 3 mice; Fig. 2D) were identical. CNQX immediately blocked the responses, which started to partially recover 40 min after washout.

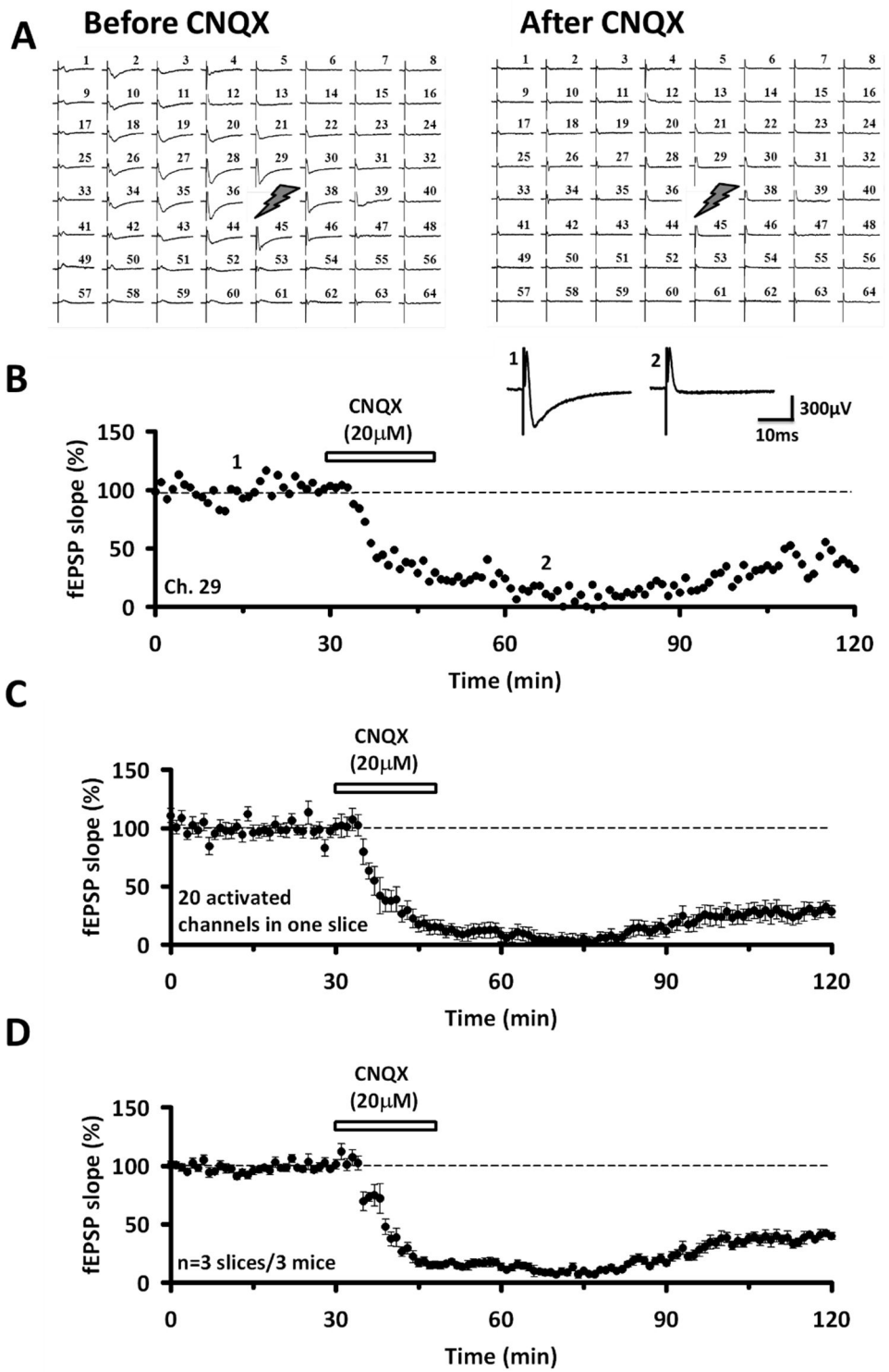
A
Before CNQX
After CNQX
B
CNQX
(20μM)
1
2
300μV
10ms
fEPSP slope (%)
Ch. 29
Time (min)
C
CNQX
(20μM)
20 activated
channels in one slice
fEPSP slope (%)
Time (min)
D
CNQX
(20μM)
n=3 slices/3 mice
fEPSP slope (%)
Time (min)

Figure 2. Glutamate-mediated synaptic transmission in the ACC

A, One sample of the fEPSPs of all channels before and after CNQX (20 μM). Channel 37 was stimulated with 9 μA (thunderbolt).

B, Result of one channel in the CNQX experiment (Channel 29). Inset traces show representative fEPSPs at the time points indicated by the numbers in the graph.

C, Summary result of 20 activated channels in one slice.

D, Summary result of in all CNQX experiments (n = 3/ 3).

Cortical depression induced by low-frequency stimulation within the ACC network

There are several LTD inducing protocols, such as low-frequency stimulation, pairing, spike-timing dependent plasticity, and by applying chemicals (Collingridge et al., 2010). We chose the low-frequency stimulation protocol (1 Hz, 15 min) for inducing LTD that has been used in various brain regions such as hippocampus, visual cortex and ACC (Dudek and Bear, 1992; Kirkwood et al., 1993; Mulkey and Malenka, 1992; Wei et al., 1999). As shown in previous reports in rat ACC (see Wei et al., 1999), low-frequency stimulation also induces a long lasting depression in the ACC of adult mice (Fig. 3A, B). However, not all activated channels underwent LTD. Therefore the average value of fEPSP slope of the activated channels in one slice showed large variation (87 ± 8 % of baseline in the last 10 min of the experiment, 20 channels in one slice; Fig. 3C). The 4-6 activated channels surrounding the stimulation site showed the highest chance of undergoing reliable LTD (75 ± 3%, n = 5/ 5; Fig. 3D).

The use of the MED64 enabled us to quantify the cortical depression in a temporo-spatial manner. This is an important advantage of this recording method because previous studies in synaptic plasticity generally select a single neuron or population of neurons to record, thus, are not able to determine the network characteristics by electrophysiology. We defined LTD in a channel if the response was depressed by at least 15% of baseline, during the last 10 min of the recording. One simple way to display the extent of LTD is by connecting the channels exhibiting LTD on a grid representing the 8 x 8 electrodes. The blue lines are the borderlines of the activated channels and the red lines are the

borderlines for LTD displaying channels for a single slice (Fig. 4A) and the pooled data (n=6/ 6; Fig. 4 B). The highest probability of observing LTD was in those channels surrounding the stimulation site. The surrounding channels in the layer II/III and V were also frequently exhibiting LTD. This could be observed by the most overlapped red region. We have also estimated the percentage of channels in these two categories. Not every activated channel went into LTD. During baseline, 30 ± 3 out of 63 channels (47 ± 5%) were activated when giving 9 μA and 13 ± 1 (20 ± 2%) channels exhibited LTD ($t_{(10)} = 5.12$, $p < 0.001$; *t* test).

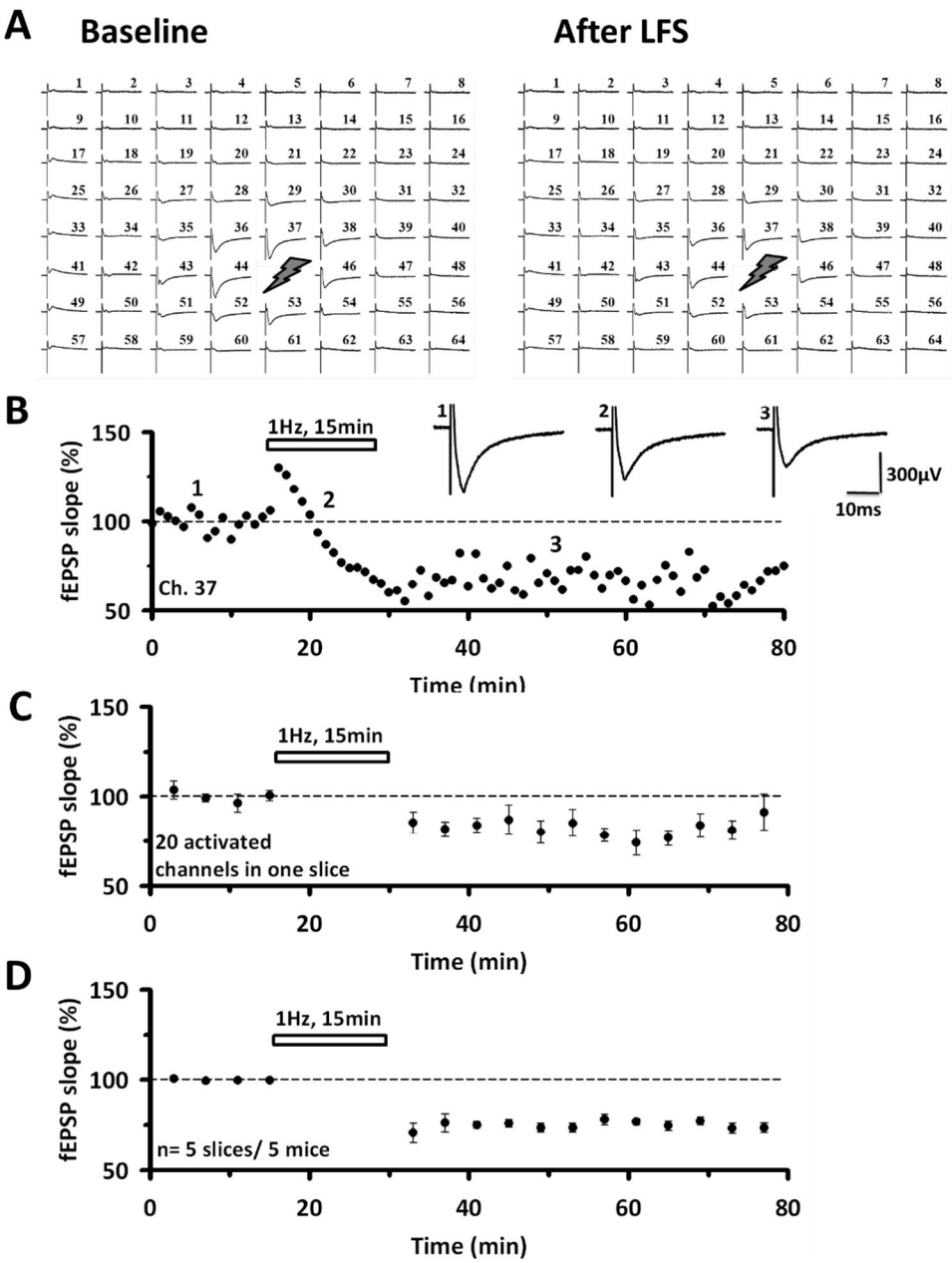
A
Baseline
After LFS
B
1Hz, 15min
fEPSP slope (%)
Ch. 37
300μV
10ms
Time (min)
C
1Hz, 15min
20 activated
channels in one slice
Time (min)
D
1Hz, 15min
n= 5 slices/ 5 mice
Time (min)

Figure 3. Low-frequency stimulation induces cortical LTD in the ACC

A, One sample of the fEPSPs during baseline (before) and 20 min after end of low-frequency stimulation (1 Hz, 15 min). Channel 45 was stimulated (thunderbolt). The amplitude of the fEPSPs in many channels decreased.

B, Result of one channel that showed LTD (Ch. 37).

C, Summary of fEPSP slope of 20 activated channels in one slice (87 ± 8%).

D, Summary data of 4-6 channels surrounding the stimulation site show more stable result (75 ± 3%; n = 5/ 5).

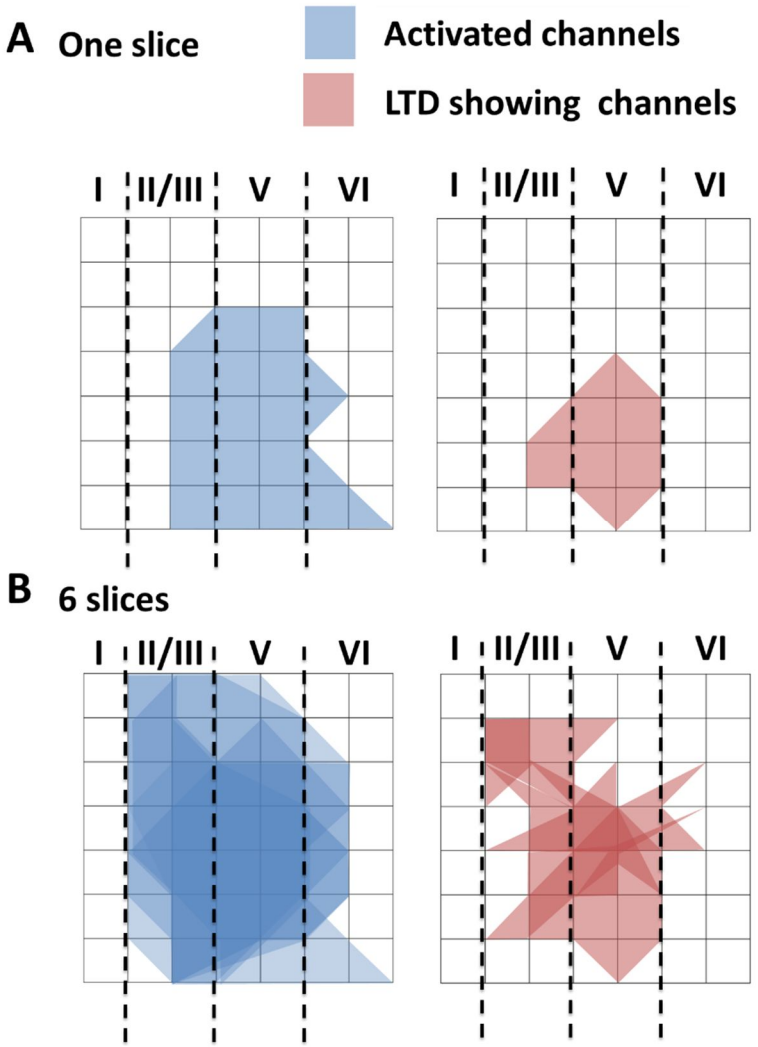

Figure 4. Spatial representation of ACC LTD

A, A polygonal diagram of the channels that were activated (blue) and that showed LTD (red). Grids represent the 64 channels in the MED64 probe. The vertical lines indicate the layers in the ACC slice.

B, Pooled data of 6 slices. The overlapped blue regions indicate frequently activated channels. The overlapped red regions indicate frequently LTD showing channels.

Frequency dependence of the induction of ACC LTD

We next investigated the frequency dependence of LTD by delivering 900 pulses at 1 Hz, 3 Hz, 5 Hz or 10 Hz. We compared the level of depression for the different induction frequencies (Fig. 5 A-E). Without giving any LTD inducing protocol, 'baseline' (101 ± 1%, n = 10/ 8, data not shown) showed stable response. 1 Hz, 15 min stimulation showed great depression (78 ± 3%, n = 8/ 8). 3 Hz, 5 min (88 ± 5%, n = 6/ 6) and 5 Hz, 3 min stimulation (92 ± 4%, n = 7/ 7) also showed some depression but not much as 1 Hz protocol. However, no depression was observed with stimulation at 10 Hz for 1.5 min (103 ± 4%, n = 6/ 6) ($H_{(4,32)}$ = 18.61, $p < 0.001$; One-way ANOVA in ranks with Dunn's post-hoc; $p < 0.05$ for baseline versus 1Hz). Therefore, we could conclude that 1 Hz is most reliable to induce LTD in the mice ACC.

We also counted the number of channels that were activated during baseline, and showed LTD (Fig. 5F). All four groups had approximately 45% activated channels. 1 Hz showed the most LTD showing channels (18 ± 3 %). 3 Hz (6 ± 2%) and 5 Hz (5 ± 3%) showed less number of LTD showing channels than 1Hz. 10 Hz (1 ± 1%) mostly did not induce any LTD throughout the 63 channels ($H_{(3,23)}$ = 15.38, p = 0.002; One-way ANOVA in ranks with Dunn's post-hoc; $p < 0.05$ for 1Hz versus 5 Hz and 10 Hz). Therefore, we could conclude that 1Hz low-frequency stimulation showed the most reliable depression out of the four frequencies examined. We also found strong linear correlation graph between depression level and number of LTD showing channels from above experiments. Fig. 5G shows a strong positive correlation between the mean depression level and

the percentage of channels displaying LTD ($r_{(25)} = 0.85$, $p < 0.001$; Pearson product moment).

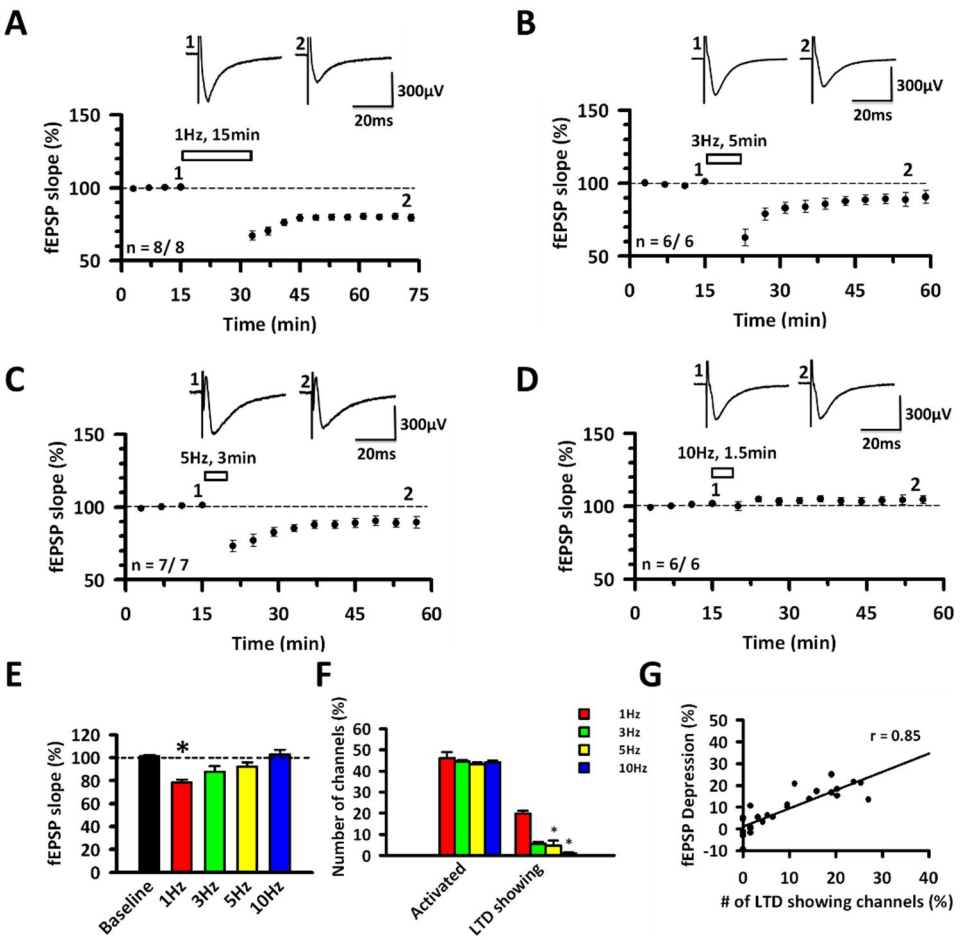
A
B
C
D
E
F
G
1Hz, 15min
3Hz, 5min
5Hz, 3min
10Hz, 1.5min
300μV
20ms
fEPSP slope (%)
Time (min)
n = 8/ 8
n = 6/ 6
n = 7/ 7
n = 6/ 6
Baseline
1Hz
3Hz
5Hz
10Hz
Number of channels (%)
Activated
LTD showing
fEPSP Depression (%)
# of LTD showing channels (%)
r = 0.85

Figure 5. Frequency dependent LTD in the ACC

A, Averaged data of LTD induced by 1 Hz, 15 min stimulation (n = 8/ 8). Averaged fEPSP slope level of the last 10 min was 78 ± 3%.

B, Averaged data of 3 Hz, 5 min for LTD induction (88 ± 5%; n = 6 /6).

C, Averaged data of 5 Hz, 3 min for LTD induction (92 ± 4%; n= 7/ 7).

D, Averaged data of 10 Hz, 1.5 min showed no depression (103 ± 4%; n = 6/ 6).

E, Summarized results of the averaged fEPSP slope level of the last 10 min following different frequencies of stimulation ($H_{(4,32)}$ = 18.61, p < 0.001; One-way ANOVA in ranks with Dunn's post-hoc; p < 0.05 for baseline versus 1Hz).

F, Summarized results of the number of channels that were activated and exhibited LTD (responses that were depressed by greater than 15%). 1 Hz showed the most LTD showing channels (18 ± 3%). 3 Hz (6 ± 2%) and 5 Hz (5 ± 3%) showed less number of LTD showing channels. 10 Hz (1 ± 1%) nearly had no LTD showing channels ($H_{(3,23)}$ = 15.38, p = 0.002; One-way ANOVA in ranks with Dunn's post-hoc; p < 0.05 for 1Hz versus 5 Hz and 10 Hz).

G, Linear correlation between fEPSP depression level and number of channels showing LTD. All four groups (1 Hz, 3 Hz, 5 Hz, 10 Hz) were used in the plot ($r_{(25)}$= 0.85, p < 0.001; Pearson product moment).

Pharmacological aspects of ACC LTD

We next defined the glutamate receptor subtypes responsible for ACC LTD using pharmacological reagents. We used the NMDA receptor antagonist AP5 (50 μM), L-type voltage gated calcium channel (L-VGCC) blocker nimodipine (10 μM), non-specific mGluR blocker MCPG (500 μM), the mGluR5 antagonist MPEP (10 μM) and the mGluR1 antagonist LY367385 (100 μM). We infused each drug for the entire experimental time (Fig. 6A-G). Control experiment with no drug showed LTD after 1Hz, 15 min low-frequency stimulation (78 ± 2%, n = 9/ 9). AP5 partially blocked the depression (88 ± 2%, n = 7/ 7), whereas both nimodipine (95 ± 3%, n = 6/ 6) and MCPG (93 ± 3 %, n = 6/ 6) blocked ACC LTD. MPEP did not affect LTD (77 ± 2%, n = 4/ 4), however, LY367385 effectively blocked LTD (96 ± 2%, n = 5/ 5) ($F_{(5,31)}$ = 10.64, $p < 0.01$; One-way ANOVA with Bonferroni post-hoc; $p < 0.001$ for control versus nimodipine, MCPG and LY367385). These results suggest that L-VGCC and mGluR1 are important for the induction of low-frequency induced ACC LTD, while action of NMDA receptor also contributes to LTD in this region.

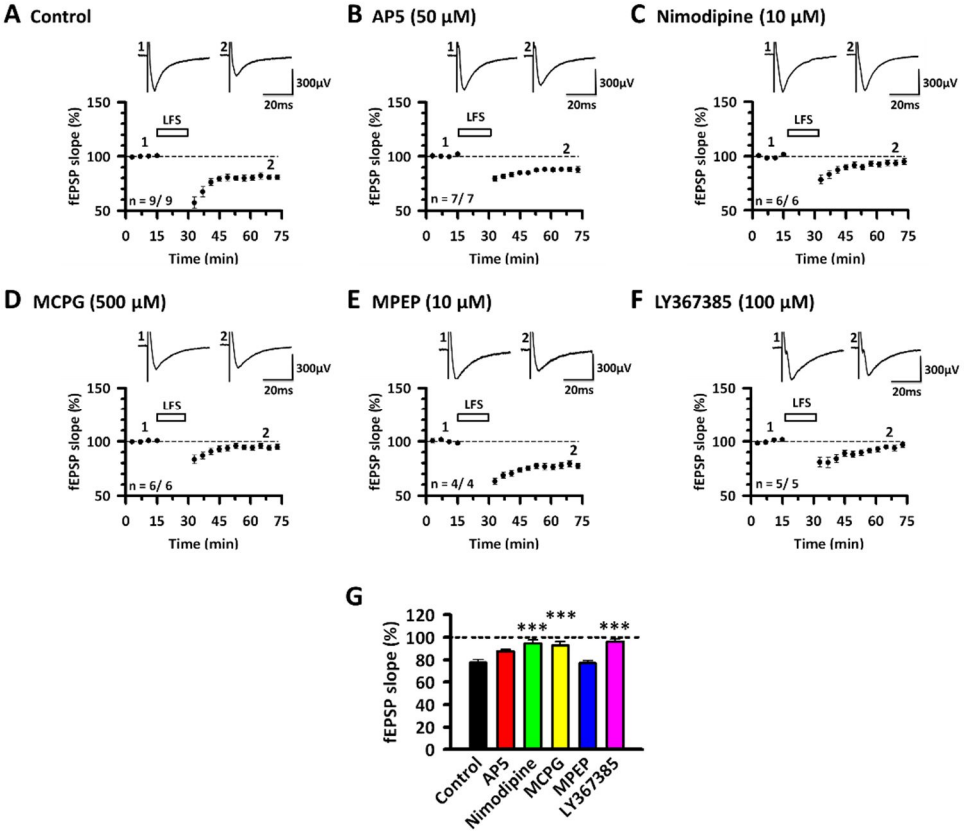
A Control
B AP5 (50 μM)
C Nimodipine (10 μM)
D MCPG (500 μM)
E MPEP (10 μM)
F LY367385 (100 μM)
G
LFS
300μV
20ms
fEPSP slope (%)
Time (min)
n = 9/ 9
n = 7/ 7
n = 6/ 6
n = 6/ 6
n = 4/ 4
n = 5/ 5
***
Control
AP5
Nimodipine
MCPG
MPEP
LY367385

Figure 6. Pharmacological aspects of ACC LTD

A, Controls showed LTD after 1Hz, 15 min low-frequency stimulation (78 ± 2%; n=9/ 9).

B, NMDA receptor antagonist, AP5 (50 μM) partially blocked LTD (88 ± 2%; n = 7/ 7).

C, L-VGCC blocker, nimodipine (10 μM) blocked LTD (95 ± 3%; n = 6/ 6).

D, Group I and II mGluR antagonist, MCPG (500 μM) also blocked LTD (93 ± 3%; n = 6/ 6).

E, mGluR5 antagonist, MPEP (10 μM) had no effect on ACC LTD (77 ± 2%; n = 4/ 4).

F, mGluR1 antagonist, LY367385 (100 μM) blocked LTD (96 ± 2%; n = 5/ 5).

G, Summarized results of the averaged fEPSP slope of the last 10 min of each experiment ($F_{(5,31)} = 10.64$, $p < 0.01$; One-way ANOVA with Bonferroni post-hoc; $p < 0.001$ for control versus nimodipine, MCPG and LY367385).

Altered ACC cortical depression after tail amputation

Recent studies show that cortical synaptic transmission undergoes long-term plastic changes after peripheral injury including amputation (Zhuo, 2008). To examine possible changes in the ACC LTD in adult mice after injury, we used the tail amputation model (Fig. 7A). Slices were prepared at 2 weeks after amputation, a time where cortical changes have been reported previously (Wei et al., 1999). Sham mice showed normal LTD (81 ± 2 %, n = 7/ 7; Fig. 7B) but in the amputated mice LTD was abolished (96 ± 2 %, n = 9/ 9; Fig. 7C). This result is consistent with the previous rat digit amputation study (Wei et al., 1999). We also checked the spatial distribution of fEPSPs within the ACC after distal tail amputation and compared this with slices from sham mice (Fig. 7D, E). There was no difference between control and amputated group with respect to the number of channels exhibiting a synaptic response to test stimulation. Layer II/III and V channels were more consistently activated than layer VI channels in both cases. However, while half of the activated channels in the control group underwent LTD, the amputated group rarely showed LTD throughout the channels.

Since the induction of ACC LTD is mGluR1 dependent, we next tested whether it was possible to induce LTD by pharmacological activation of mGluR1. To do this we applied the group 1 mGluR agonist DHPG (100 μM) together with MPEP (10 μM) so that it selectively activated mGluR1. As expected, bath application of DHPG and MPEP induced a long-lasting depression in sham mice (86 ± 4%, n = 7/ 7; Fig. 7F). However, consistent with the loss of LTD induced by electrical stimulation following tail amputation, this treatment failed to induce LTD in the amputated model (99 ± 3%, n = 8/ 8; Fig. 7G). Therefore, these

results suggest that both low-frequency stimulation induced LTD and chemical LTD are blocked throughout all the layers of ACC in the tail amputated mice. In both forms of LTD, mGluR1 was essential; thus, we selected this as the target for further experiments.

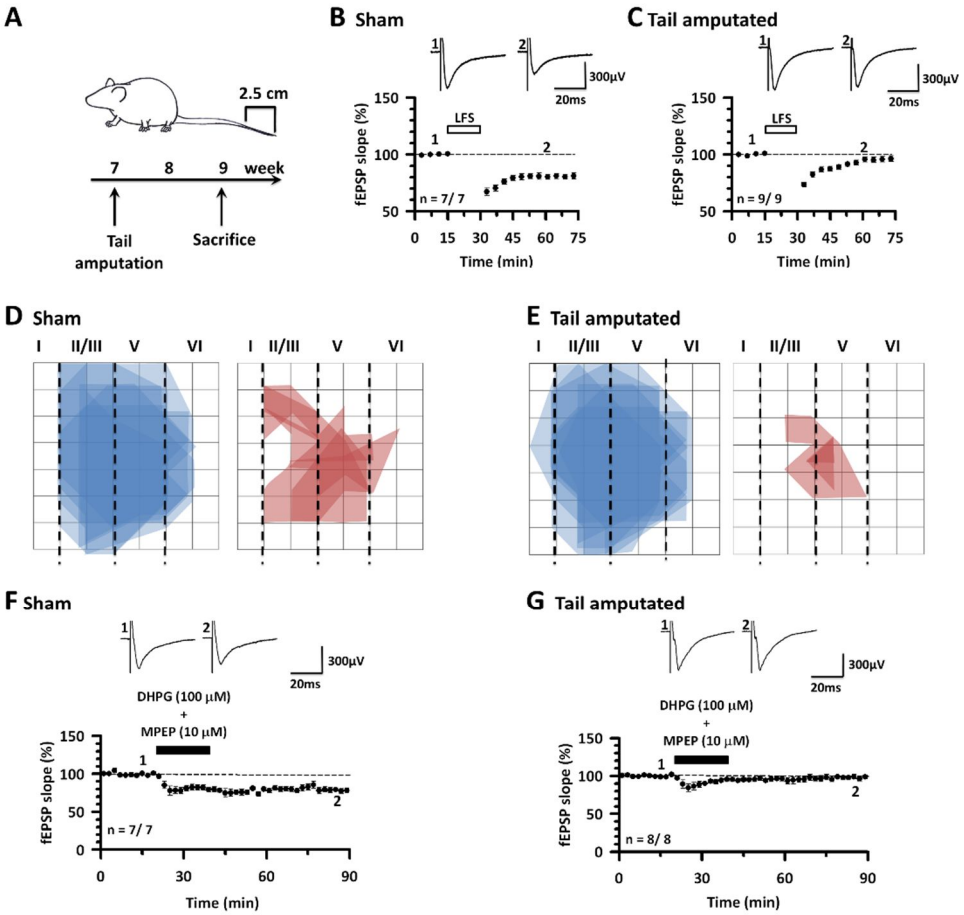
A
2.5 cm
7
8
9
week
Tail amputation
Sacrifice
B Sham
C Tail amputated
1
2
300μV
20ms
LFS
fEPSP slope (%)
150
100
50
n = 7/ 7
n = 9/ 9
0
15
30
45
60
75
Time (min)
D Sham
E Tail amputated
I
II/III
V
VI
F Sham
G Tail amputated
DHPG (100 μM)
+
MPEP (10 μM)
0
30
60
90
n = 7/ 7
n = 8/ 8

Figure 7. Tail amputation impairs ACC LTD

A, The schematic view of tail amputation experiment process.

B, The sham groups showed similar LTD as the control group (81 ± 2%; n = 7/ 7).

C, The 2 week tail amputated group showed impaired ACC LTD (96 ± 2%; n = 9/ 9).

D, E, The spatial distribution of activated channels during baseline (blue) and the channels that underwent LTD (red). The spatial distribution of activated channels during baseline in sham and amputated model is similar. However, sham group shows a wider distribution of LTD occurring channels compared with the tail amputated group, which rarely shows some LTD near the stimulation site.

F, Sham showed normal chemical LTD by applying DHPG (100 μM) and MPEP (10 μM) for 20 min (86 ± 4%; n = 7/ 7).

G, Tail amputated group showed no chemical LTD by applying DHPG (100 μM) and MPEP (10 μM) for 20 min (99 ± 3%; n = 8/ 8).

Rescuing ACC cortical depression after tail amputation

In the hippocampus, there are reports that activation of mGluRs by DHPG has a priming effect on synaptic plasticity (so-called metaplasticity), especially on LTP (Abraham, 2008; Sajikumar and Korte, 2011). We were therefore interested to see whether priming can influence the ability to induce LTD in the tail amputation model. Thus, we gave low-frequency stimulation to the slices 50 min after the end of selective activation of mGluR1 by DHPG + MPEP. While DHPG + MPEP did not induce any long-lasting depression in slices of amputated mice, subsequent low-frequency stimulation (1 Hz, 15 min) produced significant depression of fEPSPs in a single example (Fig. 8A) and in pooled data (72 ± 5%, n= 8/ 8; Fig. 8B) that was similar to that observed in sham-treated mice. This result demonstrates that the impairment of ACC LTD caused by tail amputation can be rescued by priming with the selective activation of mGluR1.

Since high concentrations of DHPG produced chemical LTD in sham slices, we decided to further test the priming effects with a lower concentration of DHPG (Fig. 8C, D). Priming with DHPG (20 μM) and MPEP (10 μM) did not produce any chemical depression in both sham and tail amputated mice ACC slices. However, subsequent low-frequency stimulation induced LTD in both sham (77 ± 6%, n = 8/ 8) and amputated animals (75 ± 5%, n = 7/ 7).

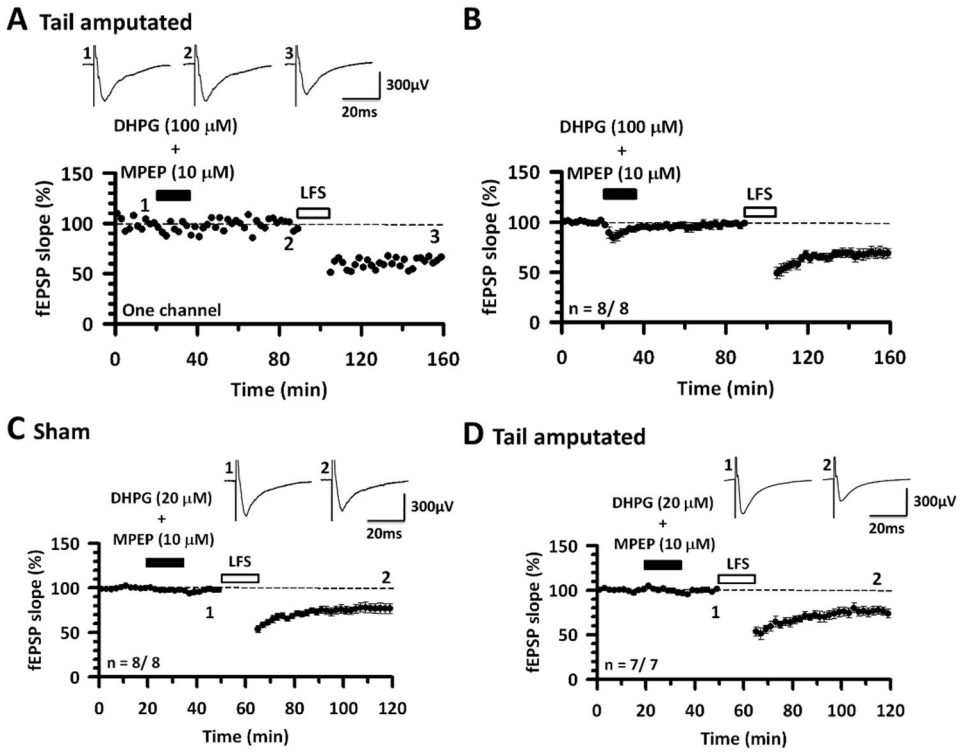

Figure 8. Recovery of ACC LTD in tail amputated mice by priming

A, B, DHPG (100 μM) and MPEP (10 μM) were given together during baseline for 20 min in the tail amputated group. After washout for 50 min, 1 Hz for 15 min low-frequency stimulation was given to induce LTD. A, Example of one channel in one slice. B, Summary data (n = 8/ 8). Amputated mice showed no depression after DHPG+MPEP (99 ± 3%) but showed depression after low-frequency stimulation (72 ± 5%; n = 8/ 8).

C, D, DHPG (20 μM) and MPEP (10 μM) were given together for 15 min in sham and tail amputated groups. After washout for 15 min, 1 Hz for 15 min low-frequency stimulation was given. C, Sham (77 ± 6%; n = 8/ 8) and D, tail amputated (75 ± 5%; n = 7/ 7) groups both showed LTD after priming.

PKC but not CaMKII or PKA is important in rescuing ACC LTD

To determine the mechanism of the metaplastic rescue in the ACC LTD, we performed pharmacological experiments using different protein kinase inhibitors (Fig. 9 A-E). Protein kinase C (PKC) and Ca^{2+}/ calmodulin-dependent protein kinase II (CaMKII) are known to be important in metaplasticity of LTP in the hippocampus (Bortolotto and Collingridge, 1998, 2000). In addition, Protein kinase A (PKA) is also implicated in hippocampal LTD and metaplasticity (Abraham, 2008; Brandon et al., 1995; Oh et al., 2006; Qi et al., 1996). Co-application of a PKC inhibitor chelerythrine (3 μM) with DHPG (20 μM) and MPEP (10 μM) during the priming period prevented the rescue of LTD in the ACC slices of amputated mice (94 ± 4%; n = 9/ 9). By contrast, inhibiting CaMKII (KN 62 (10 μM); 83 ± 3%; n = 9/ 9) or PKA (KT 5720 (1 μM); 76 ± 4%; n = 9/ 8) failed to prevent the rescue ($F_{(3,29)} = 4.70$, $p = 0.009$; One-way ANOVA with Bonferroni post-hoc; $p < 0.05$ for vehicle versus chelerythrine). These results suggest that DHPG and MPEP priming can rescue the loss of LTD in the tail amputated mice, and that PKC acts as a major factor in this process.

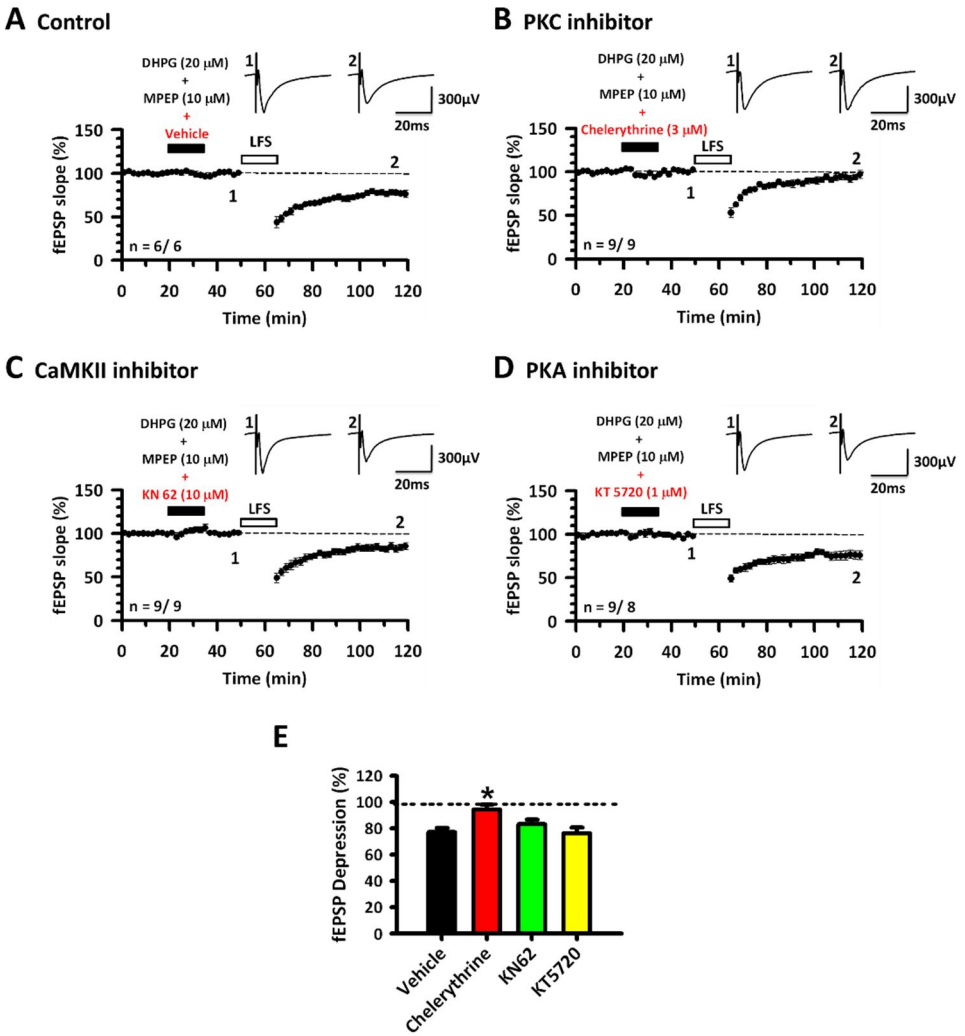
A Control
DHPG (20 μM)
+
MPEP (10 μM)
+
Vehicle
LFS
1
2
300μV
20ms
fEPSP slope (%)
n = 6/ 6
Time (min)
B PKC inhibitor
DHPG (20 μM)
+
MPEP (10 μM)
+
Chelerythrine (3 μM)
n = 9/ 9
C CaMKII inhibitor
KN 62 (10 μM)
n = 9/ 9
D PKA inhibitor
KT 5720 (1 μM)
n = 9/ 8
E
fEPSP Depression (%)
Vehicle
Chelerythrine
KN62
KT5720

Figure 9. PKC but not PKA or CaMKII is necessary for the rescue of ACC LTD

A, DHPG (20 μM), MPEP (10 μM) and each specific drug were given together for 15 min in the tail amputated mice. A, Vehicle group showed the rescue of LTD (77 ± 3%; n = 6/ 6).

B, PKC inhibitor chelerythrine (3 μM) prevented the rescue of LTD in tail amputated group (94 ± 4%; n = 9/ 9).

C, CaMKII inhibitor KN 62 (10 μM) showed depression but less than vehicle group (83 ± 3%; n = 9/ 9).

D, PKA inhibitor KT5720 (1 μM) did not prevent the rescue of LTD (76 ± 4%; n = 9/ 8).

E, Summary data of all the drugs tested in the current experiment ($F_{(3,29)} = 4.70$, $p = 0.009$; One-way ANOVA with Bonferroni post-hoc; $p < 0.05$ for vehicle versus chelerythrine).

DISCUSSION

In this study we have demonstrated that low-frequency stimulation induces LTD in the adult mouse ACC, supporting the previous report in adult rat ACC (Wei et al., 1999). Using a MEA system, we were able to show that LTD appeared in local circuits within the ACC when applying electrical stimulation to the deep layer V. The induction of LTD was frequency-dependent, with the maximal depression induced by repetitive stimulation delivered at 1 Hz. Pharmacological experiments found that LTD required the activity of mGluR1 and L-VGCCs; while inhibiting NMDA receptors only partially reduced the induction of LTD. A chemical LTD, induced by the selective activation of mGluR1 (using co-application of DHPG and MPEP), was also observed in the ACC. We found that tail amputation greatly impaired both low-frequency stimulation induced LTD and chemical LTD in the ACC. Priming ACC slices with bath application of pharmacological agents to selectively activate mGluR1 rescued the loss of LTD by amputation. Activation of PKC was required in this metaplastic LTD rescue, but activation of neither CaMKII nor PKA was required. Our results demonstrate that activation of mGluR1 in the ACC is critical for LTD, and raise the possibility that drugs that act on mGluR1 and its downstream signaling processes may help to treat phantom pain or associated brain dysfunctions.

Mapping LTD in a cortical circuit

MEA technology represents a valuable tool to record responses in

numerous sites simultaneously for a long time (Hofmann and Bading, 2006; Morin et al., 2005; Oka et al., 1999). We have used a 64-channel MEA system, MED64, in mouse brain slices to study the spatial distribution of synaptic transmission and LTD in the ACC. Within the ACC, we observed spatial distribution of excitatory synaptic transmission when stimulating deep layer V. This was the only area we could detect more than 20 channels with inward responses. Stimulating other areas, such as layer I or II/III, induced at most 10 channels of inward responses. Different responses to the test stimulation suggest that the synaptic responses we recorded are due to local synaptic networks, rather than general field responses from the same population of cells. Our results suggest, therefore, that certain local circuits in the brain slice preparation are intact. This conclusion is supported by a recent electrophysiological study using dual whole-cell patch-clamp recording technique (Wu et al., 2009). We can conclude, therefore, that neurons within different layers of the ACC are highly interconnected within the brain slice preparation. We found, however, that not every activated channel underwent LTD; the channels that are within a 300 μm radius of the stimulation site being the most likely to exhibit this form of synaptic plasticity.

Mechanisms of ACC LTD

Two major forms of LTD have been reported in the CNS; NMDA receptor-LTD and mGluR-LTD (Collingridge et al., 2010). Both forms of LTD have been reported in the ACC depending on the induction protocol. Field recording using low frequency stimulation in adult rat ACC induced mGluR-LTD (Wei et al., 1999) whereas whole-cell patch-clamp recording using a pairing

protocol in adult mouse ACC induced NMDA receptor-LTD (Toyoda et al., 2005). Depolarizing the postsynaptic neuron during the pairing protocol promotes the activation of NMDA receptor and this could give more chance to undergo NMDA receptor-LTD in the ACC. It is known that both NMDA receptor-LTD (Dudek and Bear, 1992) and mGluR-LTD (Bashir et al., 1993b) can be observed in the same type of synapse and may coexist at the same developmental stage (Oliet et al., 1997). Our present study used single shock low-frequency stimulation for LTD induction, and found that AP5 only partially inhibited ACC LTD. The depression level of the quantified channels and the number of channels that underwent LTD in the presence of AP5 were approximately half of those of the control group. However, the broad spectrum mGluR antagonist MCPG (Bashir et al., 1993a) blocked ACC LTD in terms of both the depression level and the number of channels showing LTD. These results suggest both NMDA receptors and mGluRs are involved in the ACC LTD in adult mice when repetitive low-frequency stimulation is given, but the latter have the more prominent role.

The role of group I mGluRs in synaptic plasticity has been extensively investigated in various regions of the brain. For example, at hippocampal CA1 synapses, DHPG induced LTD involves mGluR5 (Palmer et al., 1997) whereas LTD at parallel fiber to Purkinje cell synapses in the cerebellum requires mGluR1 (Conquet et al., 1994). Our study suggests that mGluR1 is the major factor for low-frequency stimulation-induced LTD in the ACC. Nimodipine also blocked low-frequency stimulation induced LTD in the ACC. Our previous reports have already shown that L-VGCCs are important for both LTD (Wei et al., 1999) and LTP (Liauw et al., 2005) in adult rodent ACC. Calcium regulation is known to be

important in synaptic plasticity and L-VGCCs provides one major route across the plasma membrane, where it is linked to gene expression (Dolmetsch et al., 2001; West et al., 2001). In addition, activation of L-VGCCs has been shown to directly facilitate the function of group I mGluRs (Rae et al., 2000). Therefore, it is not surprising to discover the role of L-VGCC in the ACC LTD, in particular one that also involves group I mGluRs.

Loss of cortical LTD after amputation

Cumulative animal and human studies demonstrate that the ACC, together with other related cortical areas, plays important roles in pain perception and chronic pain (Zhuo, 2008). Peripheral injuries, such as nerve injury or inflammation, trigger synaptic potentiation in the ACC pyramidal cells. Both presynaptic enhancement of glutamate release and postsynaptic amplification of AMPA receptor mediated responses contribute to the potentiation (Li et al., 2010; Xu et al., 2008; Zhuo, 2008). For peripheral amputation, LTP like potentiation has been reported in rats under anesthesia *in vivo* (Wei and Zhuo, 2001). Especially, *in vivo* intracellular recordings identified that LTP likely occur on excitatory synapse of cortical pyramidal cells in the ACC (Wu et al., 2005c). These studies provide a useful animal model of investigating long-term plastic changes within the cortex (or called cortical reorganization). Similar to previous studies in rats, we could not detect LTD, induced by low-frequency stimulation, within the ACC after amputation (Wei et al., 1999). Furthermore, we also observed a loss of LTD induced by the pharmacological activation of mGluR1 following amputation. In both sets of experiments we identified mGluR1 as the

subtype involved. However, our biochemical data showed that the surface level of mGluR1 was not changed after amputation compared to the sham group, suggesting that amputation triggered loss of LTD is not due to reduction of postsynaptic membrane levels of mGluR1. The modification may therefore be downstream of the receptor. Future studies are clearly needed to map this pathway. However, we cannot rule out the possibility that there was only small change of surface level of mGluR1 in some subset of ACC cells. This could have induced the major difference in ACC LTD of the amputated mice but the changes of mGluR1 level cannot be detected by our biochemical experiments.

Rescued LTD by priming with mGluRs

An unusual feature of group I mGluRs is their role in metaplasticity, where their activation can affect subsequent synaptic plasticity (Abraham, 2008). For example, in the hippocampal formation, brief prior activation of group I mGluRs has been shown to facilitate LTP (Cohen et al., 1998), to enable the induction of a pharmacologically-distinct form of LTP (Bortolotto et al., 1994) and to inhibit LTD (Wu et al., 2004). Our data suggest that low-frequency stimulation induced LTD in the ACC is more mGluR1-dependent than mGluR5. Although our biochemical data show no change in membrane expression level of mGluR1, stimulating mGluR1 could work as a rescue target in tail amputated mice LTD by activating the downstream pathway or the slightly changed surface mGluR1 in some subset of cells. We therefore applied DHPG and MPEP together to selectively activate mGluR1 in the amputated group and subsequently applied low-frequency stimulation after washout of DHPG and MPEP. To our surprise, this treatment

was able to fully restore LTD. Moreover, PKC was necessary in this metaplastic rescue. By contrast, neither CaMKII nor PKA is required. Consistent with previous studies in the hippocampus (Bortolotto and Collingridge, 2000), PKC is required for metaplasticity of LTD in the ACC. Future studies are needed to identify the role of specific subtypes of PKC in this form of metaplasticity. In contrast to the metaplasticity of LTP in the hippocampus (Bortolotto and Collingridge, 1998), we found CaMKII was not required for this form of metaplasticty in the ACC though its inhibition did tend to reduce the level of priming. Moreover, a recent study showed in the hippocampus that CaMKII was important in mediating DHPG-induced mGluR-LTD but not PKC (Mockett et al., 2011). These results indicate that intracellular mechanisms mediated by priming group I mGluR in LTD maybe dose related and region dependent.

In summary, we have used a MEA approach to investigate the spatial distribution and the cortical circuitry involved in the mouse ACC and found that LTD was expressed in a network-dependent manner. Low-frequency stimulation induced LTD in the ACC required the activation of both mGluR1 and L-VGCCs. In tail amputated mice, LTD was greatly reduced in all the ACC layers, but could be fully rescued by the transient pharmacological activation of mGluR1 via a priming mechanism involving PKC.

CHAPTER III

Bidirectional modulation of hyperalgesia via the specific control of excitatory and inhibitory neuronal activity in the ACC

INTRODUCTION

The role of the anterior cingulate cortex (ACC) in pain conditions has been consistently demonstrated for the past several decades (Vogt, 2005; Zhuo, 2008). Human brain imaging studies report responses of the ACC, and related cortical areas, to acute nociceptive stimuli (Dunckley et al., 2005; Peyron et al., 2000; Strigo et al., 2003; Talbot et al., 1991). Moreover, surgical lesions of the cingulate cortex (cingulotomy) reduced the unpleasantness of pain (Pillay and Hassenbusch, 1992; Wong et al., 1997; Yen et al., 2009; Yen et al., 2005). Given the important role of ACC in pain, numerous animal studies have been performed in this region to reveal the pathways and molecular mechanism of nociception and chronic pain(Fuchs et al., 2014; Shyu and Vogt, 2009; Zhuo, 2011). For example, lesion in rat ACC, similar to human cingulotomy, reduced aversive behavior during the conditioned place aversion test (Johansen et al., 2001), and escape/avoidance test (LaGraize et al., 2004). Numerous electrophysiological studies have also observed increased activation of the ACC in both acute and chronic pain situations. For example, an acute nociceptive stimulus in the peripheral region induced increased firing of ACC pyramidal neurons whereas a brush stroke had minimal effect(Koga et al., 2010; Shyu et al., 2008; Sikes and Vogt, 1992). Peripheral injury induced long-term potentiation (LTP) of excitatory synaptic responses in the ACC neurons (Wei and Zhuo, 2001; Xu et al., 2008). Pharmacological inhibition or genetic deletion of LTP related molecules in the ACC reduced pain in chronic models (Li et al., 2010; Wang et al., 2011; Wei et al., 2002; Wu et al., 2005a). Furthermore, using pharmacological

manipulations and electrical stimulation within the ACC, it has been shown that ACC activation can elicit aversive behaviors (Calejesan et al., 2000; Chen et al., 2014b). Yet, the spatiotemporal precision of ACC neuronal activity in pain remains enigmatic and the function of different ACC neuronal subtypes is controversial.

Optogenetic tools are increasingly being used to identify the neural circuits underlying various types of behaviors or to reveal the functions of specific subtypes of cells (Tye and Deisseroth, 2012; Yizhar et al., 2011). Several cre line mice are available for the selective manipulation of specific cell types (Van den Oever et al., 2013; Wolff et al., 2014). However, these methods have only just started to be applied to the understanding of pain pathways. Studies to date have been performed in peripheral regions (Iyer et al., 2014), brain stem (Hickey et al., 2014), medial prefrontal cortex (mPFC)(Lee et al., 2015; Wang et al., 2015; Zhang et al., 2015) and ACC (Barthas et al., 2015; Gu et al., 2015). The two optogenetic studies in the ACC used Thy1-ChR2 mice, which expresses ChR2 indiscriminately within excitatory and inhibitory neurons. One group reported that activation of ACC showed anxiodepressive-like behaviors but no change in pain (Barthas et al., 2015). However, the other group observed an alleviation of acute inflammatory pain (Gu et al., 2015) which they attributed to the activation of inhibitory interneurons. The reason for these discrepant results is unknown.

In the present study, we used optogenetics and cre- expressing mouse lines to, for the first time, specifically manipulate the activity of excitatory neurons

and interneurons within the ACC to establish whether specific neuronal subtypes within this brain region can acutely modulate nociceptive responses. We injected channelrhodopsin-2 (ChR2) or halorhodopsin (eNpHR3.0) carrying adeno-associated virus (AAV) in CaMKII-cre mice to activate or inhibit, respectively, the CAMKII-expressing ACC excitatory neurons. We also injected ChR2 into PV-cre or SOM-cre mice to activate specific PV positive or SOM positive interneurons. We found that activation of ACC pyramidal neurons decreased the basal mechanical threshold but did not further decrease the level in CFA-treated mice. In contrast, inhibition of these neurons reversed the effects of CFA treatment without affecting the basal mechanical threshold. Moreover, activation of PV-type interneurons, but not SOM-type interneurons, also alleviated the CFA-induced pain hypersensitivity. These results show that excitatory neurons within the ACC are both necessary and sufficient for nociceptive processing and that they are under tight regulation by PV-expressing interneurons. These results suggest that ACC excitatory neurons are one of the critical mediators of nociception.

EXPERIMENTAL PROCEDURES

Animals

Adult (8-12 week old) male CaMKII-, PV- or SOM- cre mice (Jackson Laboratory) were used. All animals were housed under a 12 h light/dark cycle with food and water provided *ad libitum*. All works were conducted according to the policy and regulation for the care and use of laboratory animals approved by Institutional Animal Care and Use Committee at Seoul National University.

Stereotaxic virus injection, Optic cannula implantation

AAV carrying DIO-ChR2-EYFP, DIO-eNPHR3.0-EYFP or DIO-EYFP constructs was injected into 6 week-old CaMKII-cre hetero male mice. PV-cre hetero and SOM-cre hetero or wild-type littermates (control) were also injected with AAV-DIO-ChR2-EYFP. Mice were anesthetized with an intraperitoneal injection of ketamine-xylazine (0.1mg per gram body weight ketamine, 0.01 mg per gram body weight xylazine) and the head was fixed in a stereotaxic apparatus (Kopf Instruments, Tujunga, CA, USA). A small craniotomy was performed and, five holes were drilled. Two holes were drilled bilaterally between the hippocampus and cerebellum for screw implantation. The other three holes were drilled for virus injection and optic cannula implantation in the ACC. The virus was delivered using a 10 μl syringe (Hamilton) and a 30 gauge metal needle. The injection volume and flow rate (0.5 μl at 0.1 μl/min) were controlled by an injection pump (WPI). Virus was injected into both side of the ACC (anteroposterior [AP] + 1.0 mm from bregma, mediolateral [ML] ± 0.35 mm,

dorsoventral [DV] -2.2 mm). After injection, the needle was left for additional 7 min and then was slowly removed. The optic cannula (MFC_200/230-0.39_2mm_ZF1.25_FLT, Doric Lenses., Quebec, Canada) was implanted between the virus injection site (AP + 1.0 mm from bregma, ML + 0 mm, DV – 1.25 mm). The optic cannula was then fixed with dental cement.

Behavior

Electrical von Frey system for checking the mechanical nociceptive of withdrawal threshold

A pre-test was done 3 weeks after the surgery and CFA (1:1 mixture with saline) or saline 10 μl was injected in the hind paw after the test. 3 days later the post-test was performed. In each test, there were three light 'off' and two light 'on' sessions (off1-on1-off2-on2-off3, 5 min intersession interval). Paw withdrawal threshold was measured with the electronic von Frey system. The averages of three values were calculated as the threshold of that session. 593 nm light was given continuously in an intensity of 7-9 mW/cm^2. 473 nm light was given at 10 Hz (40 ms pulse) throughout the 'on' period for the CaMKII-cre mice. PV-cre and SOM-cre mice were given 473 nm light in 300 ms pulses with 2 s inter-pulse intervals. An intensity of 20-25 mW/cm^2 at fiber tip was used in all ChR2 experiments.

Electrophysiology

Patch clamp recording

For whole-cell patch clamp recording, 300 μm thick coronal slices of ACC were prepared with a Leica VT-1000S slicer and incubated in artificial cerebrospinal fluid (aCSF) at 25~26°C for 1 h. The aCSF comprised 124 mM NaCl, 2.5 mM KCl, 1 mM NaH_2PO_4, 25 mM $NaHCO_3$, 10 mM Glucose, 2 mM $CaCl_2$, 2 mM $MgSO_4$ was used for the incubation and bath solution. The bath solution was oxygenated with 95% CO_2, 5% O_2 mixed gas and perfused 2 ml/min at 25~26°C (TC-324B, Warner). The slices were transferred to the recording chamber of a BX51WI microscope (Olympus) and visualized with a ProgRes MFcool CCD camera.

For current-clamp recording, the borosilicate glass recording pipettes were filled with internal solution containing 145 mM K-gluconate, 5 mM NaCl, 0.2 mM EGTA, 10 mM HEPES, 2 mM MgATP, 0.1 mM Na_3GTP, 1 mM $MgCl_2$ (pH 7.2 with KOH, 280~290 mOsm). For current injection, pyramidal neurons in layer 2/3 were current clamped and 20 pA-140 pA depolarizing current was injected for 10 s while 473 nm light was delivered to the ACC area using a 300 ms pulse width and 2 s inter-pulse interval. For pulse train experiments, pyramidal neurons in layer 2/3 were current clamped and 2 Hz depolarizing current pulses (80 pA pulse with 200 ms width) were injected for 90 s. 473 nm light was delivered to the ACC area using 300 ms pulses with a 2 s inter-pulse interval for 30 s in the middle of the trains.

In-vivo recording

After 3 weeks of recovery, the mice was anesthetized with urethane (Sigma, 0.13 g/100 g) injection and the head was fixed in a stereotaxic apparatus (Kopf Instruments, Tujunga, CA, USA). A small craniotomy was performed and two holes were drilled above the ACC on each side of the brain (AP + 1.0 mm from bregma, ML ± 0.0 mm) and a third was drilled in the cerebellum for reference. A customized optrode, composed of a tungsten electrode (A-M Systems, USA) and optic cannula (MFC_200/230-0.39_50mm_ZF1.25_FLT, Doric lenses, USA), was inserted into the ACC for multiunit recording. Neural activity was amplified 1000 fold and digitized (sampled at 32 kHz, filtered at 600-6000 Hz) using a Digital Lynx data acquisition system (Neuralynx).

Immunohistochemistry

Mice were perfused with 4% paraformaldehyde (PFA) in PBS and then brains were sectioned into 50 μm slices with Cryostat. Next, we washed slices 3 times with PBS shaking in 150 rpm for 5 min at room temperature. Slices were blocked and permeablized with 5 % goat serum, 0.2 % Triton-X 100 in PBS shaking in 80 rpm for 1 h at room temperature. Rabbit anti-somatostatin antibody (1:500, Bachem, T-4103) and mouse anti-parvalbumin antibody (1:1000, Sigma, P3088) were diluted in the blocking solution and the slices were agitated for overnight at 4°C.

Next day, slices were washed 3 times with PBS shaking in 150 rpm for 5 min at room temperature. Goat anti-rabbit IgG, Alexa Fluor® 546 conjugate (1:300, Invitrogen, A11035) and goat anti-mouse IgG, Cy5 conjugate (1:300) were diluted in the blocking solution and the slices were treated with the blocking solution

shaking in 80 rpm for 2 h at room temperature. Once again, slices were washed 3 times with PBS shaking in 150 rpm for 5 min at room temperature and mounted with VECTASHIELD® Mounting Media (Vector Laboratories) on slide glasses.

Data analysis

All data are presented as mean ± SEM. Statistical comparisons were made using the *t*-test, one-way and two-way ANOVA by SigmaPlot 11.0. The post hoc Bonferroni test was used for further comparison. If the data did not pass the equal variance test, one way ANOVA was done in ranks and Dunn's method was used for post-hoc test. In all cases, statistical significance was indicated by * $p < 0.05$.

RESULTS

Discrete cellular population in the ACC and manipulation of the excitatory neurons

In the present study, we used three cre mouse lines (CaMKII-, PV-, SOM-cre) for optogenetic manipulation in the ACC. We performed immunostaining in the ACC to observe the distribution of these three different molecular targets. AAV-DIO-EYFP was injected bilaterally into the ACC of CaMKII-cre mice and PV and SOM were stained with antibodies (Fig. 10A). All three markers were expressed throughout the ACC but within discrete cellular populations.

We next tested the effectiveness of the rhodopsins in pyramidal neurons within the ACC. AAV-DIO-eNpHR3.0, AAV-DIO-ChR2 or AAV-DIO-EYFP were injected into the ACC of CaMKII-cre mice and multiunit in vivo recording using an optrode was performed 3 weeks later. Activation of ChR2 with blue (473 nm) light stimulated the ACC neurons whereas activation of eNpHR3.0 with yellow (593 nm) light inhibited their activity (Fig. 10B).

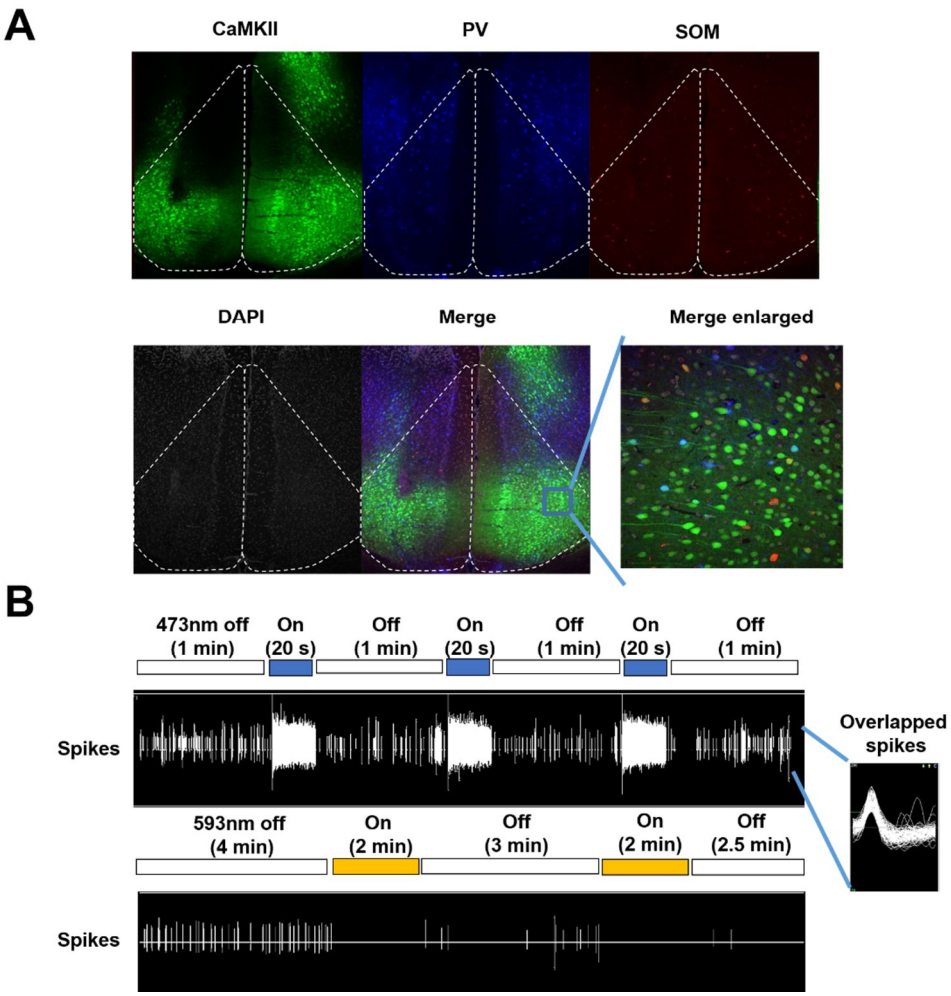
A
CaMKII
PV
SOM
DAPI
Merge
Merge enlarged
B
473nm off
(1 min)
On
(20 s)
Off
(1 min)
On
(20 s)
Off
(1 min)
On
(20 s)
Off
(1 min)
Spikes
Overlapped
spikes
593nm off
(4 min)
On
(2 min)
Off
(3 min)
On
(2 min)
Off
(2.5 min)
Spikes

Figure 10. Distinct cell populations and viral expression of rhodopsins in the ACC of CaMKII-cre mice

A, Tissue staining of three different markers in the ACC. AAV-DIO-EYFP was injected to ACC of CaMKII-cre mice. CaMKII (EYFP), PV and SOM do not co-localize in the ACC. Dotted polygons indicate one side of ACC.

B, Optogenetic modulation during multiunit *in vivo* recording in the ACC of anesthetized mice. 473 nm light stimulated the basal firing of CaMKII-cre mice injected with AAV-DIO-ChR2-EYFP and 593 nm light inhibited the basal firing of CaMKII-cre mice injected with AAV-DIO-eNpHR-EYFP.

Activation of excitatory neurons in the ACC decreases the mechanical threshold

Throughout our study, we injected AAV-DIO-ChR2, AAV-DIO-eNpHR3.0 or AAV-DIO-EYFP in the ACC bilaterally and the optic cannula was implanted in the middle of the viral injection sites (Fig. 11A). We first tested whether specific activation of ACC excitatory neurons is itself sufficient to modulate the nociceptive responses. To address this question, AAV-DIO-ChR2 was injected into the ACC of CaMKII-cre mice (CaMKII-ChR2) and 473 nm light was pulsed at 10 Hz throughout the 'ON' period for ACC activation. This frequency was selected according to the previous *in vivo* whole-cell patch recording data in the ACC during noxious stimulation (Koga et al., 2010). Interestingly, the mechanical threshold of the majority (10/18) of the mice decreased when the light was given and fully recovered back to the baseline value when the light was turned off (Fig. 11B, D). This effect was replicated when a second period of light excitation was employed (Fig. 11B, D). In contrast, the AAV-DIO-EYFP injected control group was invariably unaffected by light (Fig 11B) [EYFP (off: 4.99±0.22 g, on: 4.81±0.22 g; n = 10) and ChR2 (off: 4.90±0.13 g, on: 4.12±0.22 g; n = 18; Fig. 11C)]. The 'off' and 'on' sessions were averaged for statistical analysis and there was a statistically significant interaction between light ('off' and 'on') and virus ('ChR2' and 'EYFP') infused ($p = 0.011$, two-way repeated measures ANOVA). There was no difference in the patterns of ChR2 expression between the "decrease" and "non-decrease" groups (Fig. 11E).

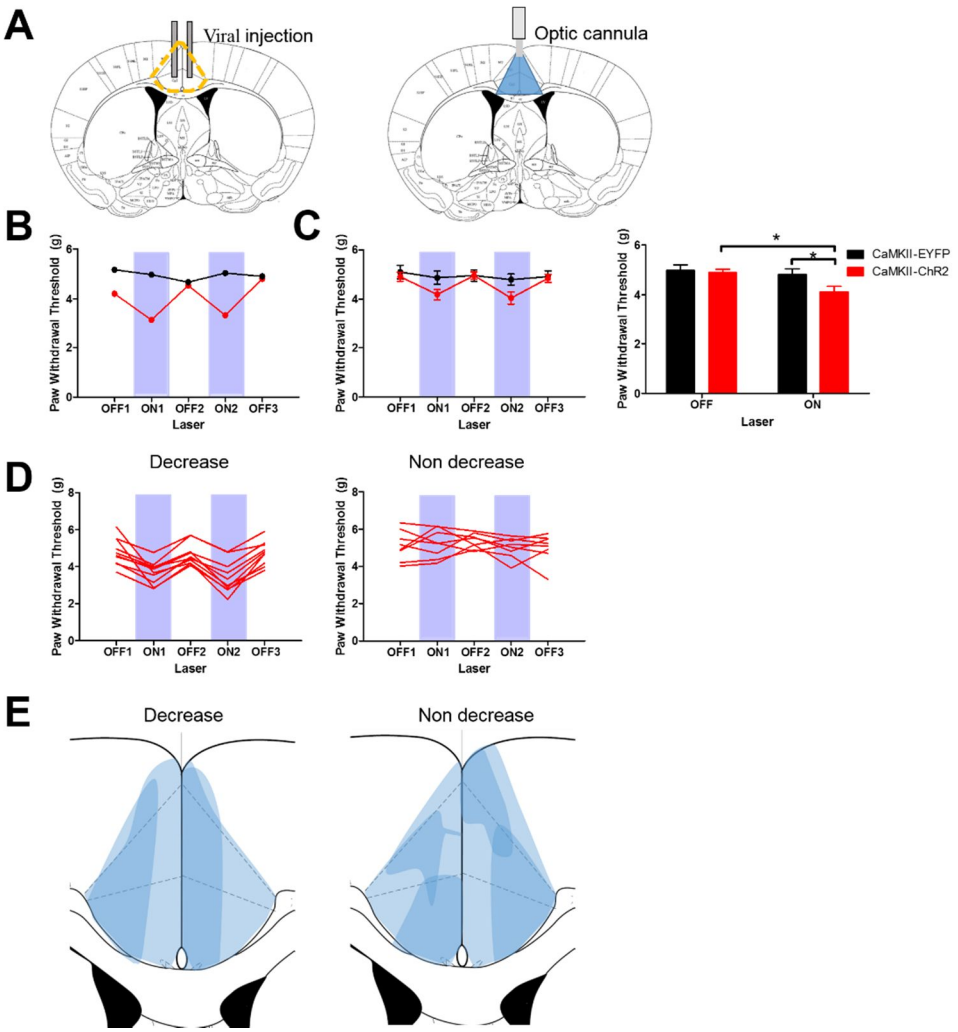
A
Viral injection
Optic cannula
B
C
Paw Withdrawal Threshold (g)
OFF1 ON1 OFF2 ON2 OFF3
Laser
OFF ON
CaMKII-EYFP
CaMKII-ChR2
D
Decrease
Non decrease
E
Decrease
Non decrease

Figure 11. Activation of CaMKII-positive neurons in the ACC decreases the mechanical threshold.

A, Schematic diagram of viral injection site (left) and, optic cannula placement (right) in the ACC.

B, One example of the effects of blue light in a CaMKII-ChR2 expressing mouse (red) and an EYFP expressing mouse (black) in the von Frey test.

C, Pooled data for ChR2 and EYFP mice. On average there was a reduction in the mechanical threshold in the ChR2 group. The graph on the right plots the combined data for the two ON and three OFF episodes. There was a significant effect of laser light in the ChR2 group: Off: 4.90±0.13 g, on: 4.12±0.22 g; n = 18) but not in the EYFP group (off: 4.99±0.22 g, on: 4.81±0.22 g; n = 10) [p = 0.011 in virus and light interaction, two-way repeated measures ANOVA].

D, Not all animals showed a decrease of the mechanical threshold during light activation. Out of 18 animals, 10 showed a decrease whilst 8 did not.

E, The overlapped pattern of ChR2 expression in each group.

Activation of ACC excitatory neurons has no effect in chronic pain conditions

To examine the role of ACC excitatory neurons in chronic pain condition, we used CFA treatment and performed behavioral experiments as shown schematically in Fig. 12A. In contrast to the effects of activating ACC excitatory neurons of CaMKII-ChR2 mice in a non- painful situation (Before CFA; off: 5.00±0.23 g, on: 4.13±0.40 g; n = 8; Fig. 12B black), there was no modification of the mechanical threshold in the chronic pain state (After CFA; off: 3.25±0.25 g, on: 3.29±0.28 g; n = 8; Fig. 12B red). This suggests an occlusion of the effects of optogenetic activation of excitatory ACC neurons and the effects of inflammatory pain-induced signals. In the saline injected control group, there was a similar light-induced reduction in the pain threshold both before (off: 4.83±0.15 g, on: 4.12±0.25 g; n = 10; Fig. 12C green) and after saline (off: 4.54±0.11 g, on: 4.08±0.23 g; n = 10; Fig. 12C blue) injection. There was no light effect in control groups (Fig. 13).

To test the effects of ChR2 activation on locomotion and anxiety we performed an open field test (OFT). These results identify excitatory ACC neurons as effectors of pain responses and show that their activation alone is sufficient for a significant alteration in the mechanical pain threshold.

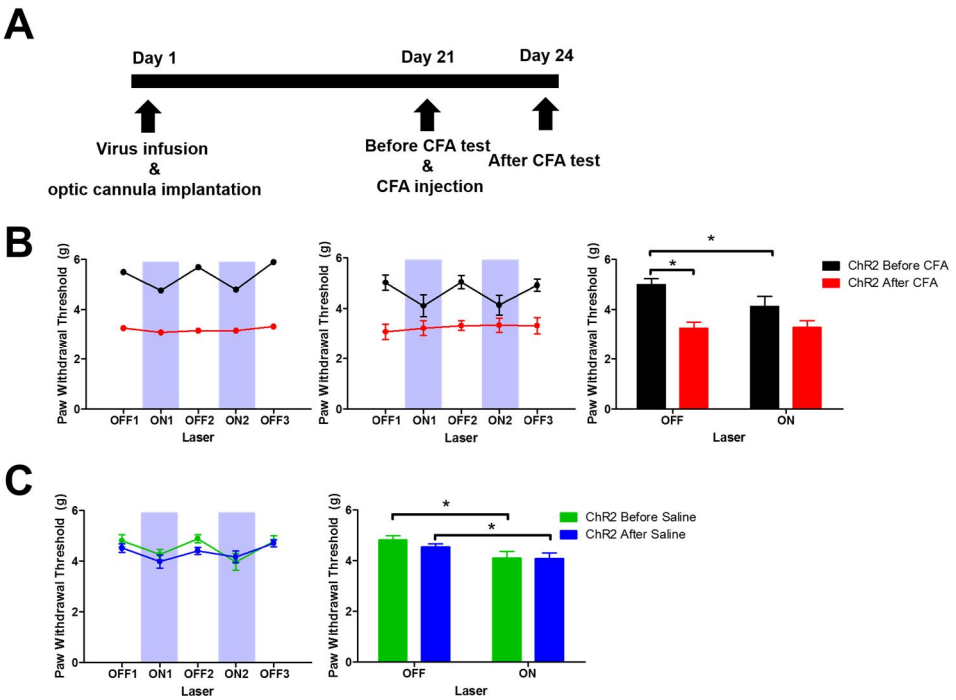
A
Day 1
Day 21
Day 24
Virus infusion
&
optic cannula implantation
Before CFA test
&
CFA injection
After CFA test
B
Paw Withdrawal Threshold (g)
OFF1 ON1 OFF2 ON2 OFF3
Laser
OFF ON
ChR2 Before CFA
ChR2 After CFA
C
ChR2 Before Saline
ChR2 After Saline

Figure 12. Activation of CaMKII-positive neurons in the ACC has no effect on the mechanical threshold in CFA-treated mice.

A, Schematic of the behavioral experiment. The pre-test was performed three weeks after the virus infusion and optic cannula implantation. After the pre-test, CFA or saline was injected into the sole of the right hind paw. The post-test was done three days after the CFA injection.

B, Effects of blue light in a ChR2 mouse (left) and pooled data (right) before (black) and after (red) CFA treatment. There was significant effect of 473nm laser before CFA (off: 5.00±0.23 g, on: 4.13±0.40 g; n = 8). CFA injection resulted in a lowering of the mechanical threshold and blue light had no effect (off: 3.25±0.25 g, on: 3.29±0.28 g; n = 8) [$p < 0.001$ in CFA, $p = 0.108$ in laser, $p = 0.120$ in CFA and light interaction, two-way repeated measures ANOVA].

C, Equivalent results for the saline treated group. There was a significant effect in both the pre-test (off: 4.83±0.15 g, on: 4.12±0.25 g; n = 10) and post-test (off: 4.54±0.11 g, on: 4.08±0.23 g; n = 10)[$p = 0.128$ in saline, $p = 0.027$ in laser, $p = 0.445$ in saline and light interaction].

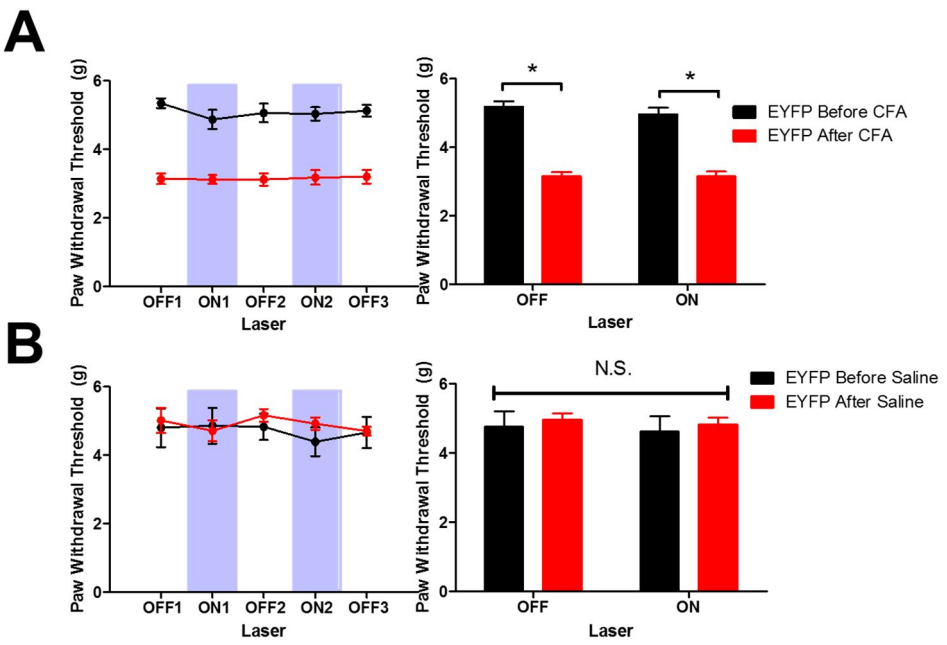

Figure 13. Control data of optogenetic activation on ACC CaMKII-positive neurons.

A, Result of the CaMKII-EYFP-CFA group. There was no light effect during either the pre-test (off: 5.18±0.17 g, on: 4.96±0.19 g; n = 7) or the post-test (off: 3.15±0.12 g, on: 3.15±0.14 g; n = 7). There was only statistically significant effect of CFA treatment *per se* ($p < 0.001$, two-way repeated measures ANOVA).

B, Result of CaMKII-EYFP-Saline group. There was no light effect either before (off: 4.77±0.44 g, on: 4.63±0.44 g; n = 6) or after saline injection (off: 4.96±0.17 g, on: 4.82±0.22 g; n = 6).

Inhibition of excitatory neurons in the ACC reverses the effects of inflammatory pain

We next inhibited ACC excitatory neurons, expressing eNpHR3.0 (CaMKII-eNpHR), with yellow light and determined the mechanical threshold before and 3 days after CFA treatment. Interestingly, optogenetic illumination had no effect on the mechanical threshold before CFA injection (off: 4.94 ± 0.22 g, on: 4.90 ± 0.36 g; n = 9) but after CFA treatment it reversed the mechanical pain threshold to near control values (3.05 ± 0.19 g, on: 4.16 ± 0.24 g; n = 9; Fig. 14A). The effect of optogenetic illumination was fully reversible and repeatable. Thus, optogenetic inhibition of excitatory neurons in the ACC substantially reversed the increase of mechanical sensitivity in the chronic inflammation pain model ($p = 0.011$ in drug and light interaction, two-way ANOVA repeated measures). In contrast, there was no effect of light in the saline injection group (Fig. 14B). Comparison of the light 'ON' phases for all four groups showed statistically significant differences between the groups ($p < 0.001$, one-way ANOVA), such that the EYFP-CFA group was significantly different from the other groups (Fig. 14C).

To test for the specificity of excitatory neurons within the ACC for the modulation of the pain threshold, we examined the effects of light on CaMKII-eNpHR neurons within the retrosplenial cortex (RSG), a region adjacent to the ACC. In contrast to the ACC, yellow light had no effect on pain thresholds (Fig. 15). These result shows that transient inhibition of excitatory neurons in the ACC can significantly reverse the enhanced sensitivity to a mechanical stimulus caused by inflammation. This suggests, therefore, that excitatory neurons in the ACC may be effectors of the sensation of pain.

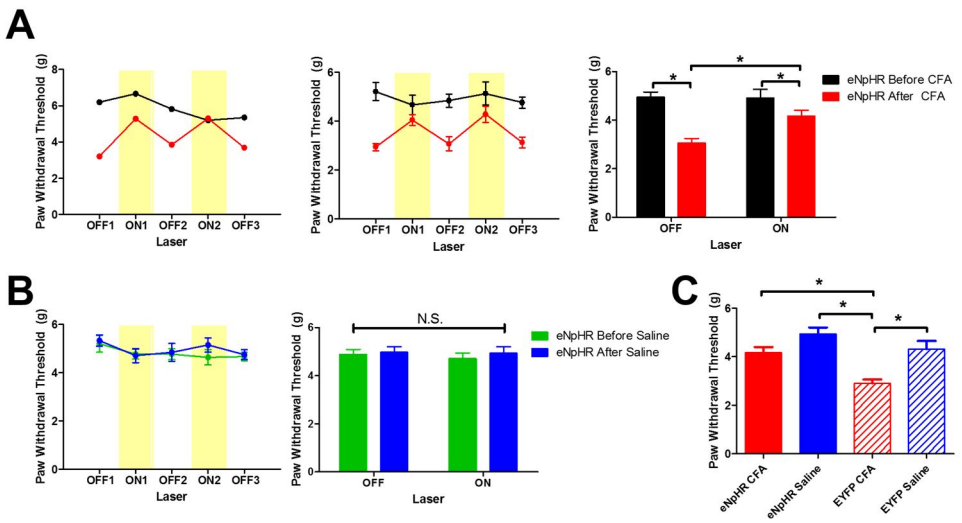

Figure 14. Inhibition of CaMKII-positive neurons in the ACC alleviates the CFA-induced decrease of the mechanical threshold.

A, Results of the eNpHR-CFA group. There was no effect of yellow light before CFA (off: 4.94±0.22 g, on: 4.90±0.36 g; n = 9). However, the mechanical threshold was increased when light was given after CFA injection (off: 3.05±0.19 g, on: 4.16±0.24 g; n = 9) [p = 0.011 in CFA and laser interaction, two-way repeated measures ANOVA].

B, Result of eNpHR-Saline group. There was no light effect before (4.88±0.21 g, on: 4.71±0.24 g; n = 7) and after saline (off: 4.98±0.23 g, on: 4.93±0.27 g; n = 7).

C, Comparison of the post-test light 'on' period in all four groups. There was statistically significant difference between groups ($p < 0.001$, one-way ANOVA).

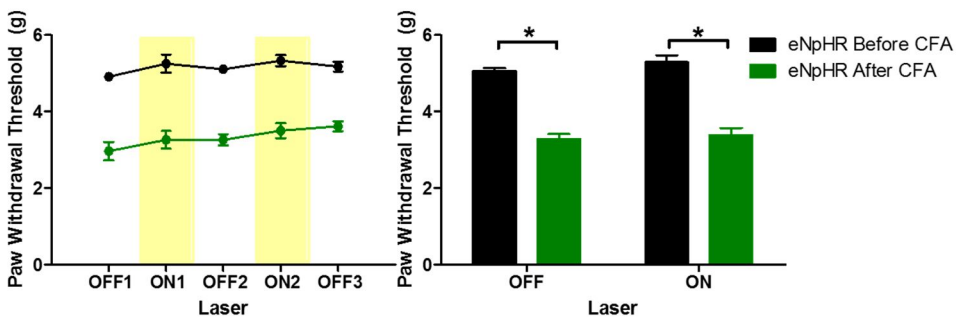

Figure 15. Optogenetic inhibition of CaMKII-positive neurons in the RSG.

There was no light effect either before (off: 5.07±0.07 g, on: 5.29±0.18 g; n = 8) or after CFA injection (off: 3.28±0.13 g, on: 3.38±0.19 g; n = 8).

Optogenetic activation of inhibitory neurons in the ACC reverses the effects of inflammatory pain

The ACC comprises both excitatory neurons and a diverse array of inhibitory neurons that may play distinct roles in the modulation of pain thresholds. A major class of GABAergic inhibitory neurons expresses parvalbumin (PV). We therefore tested whether activation of the ACC PV-positive interneurons could modulate the mechanical threshold during chronic inflammation pain. 473 nm light was given at 0.5 Hz throughout the ON period, using a protocol previously applied to the amygdala (Wolff et al., 2014). We found that activation of PV-ChR2 expressing neurons could substantially alleviate CFA-induced pain. In the PV-ChR2 group there was no significant effect of the 473 nm light before CFA (off: 5.30 ± 0.15 g, on: 5.04 ± 0.07 g; n = 6). However, there was significant increase in the mechanical threshold after CFA injection (off: 3.44 ± 0.11g, on: 4.55 ± 0.21g; n = 6; Fig. 16A; $p = 0.002$ in CFA and light interaction, two-way repeated measures ANOVA). Since the behavioral outcome is similar to that of the CaMKII-eNpHR mice, we wondered whether PV optogenetic activation will inhibit excitatory neurons. Current injection and pulse train tests were performed using whole-cell patch-clamp recording and light was given at 0.5 Hz to mimic the behavioral experiments with the PV-ChR2 mice. In the current injection experiment, (Fig. 16B, right), excitatory neurons showed a greater decrease of firing in the light group compared to the control group (Fig. 16B, left). Moreover, in the pulse train test, the firing of excitatory neurons were reduced during the light presentation and recovered when the illumination was stopped (Fig. 16C). These

results demonstrate that optogenetic excitation of PV+ interneurons inhibits the activity of ACC pyramidal neurons.

In contrast to the effects of activation of PV+ interneurons, there was no effect of the illumination of SOM-ChR2 expressing neurons on the mechanical threshold either before (off: 5.11 ± 0.15 g, on: 4.95 ± 0.11 g; n = 12) or after CFA treatment (off: 3.32 ± 0.16 g, on: 3.30 ± 0.13 g; n = 12; Fig. 16D). The whole-cell patch-clamp experiments also showed minimal effect of optogenetic excitation of SOM+ interneurons on the activity of ACC pyramidal neurons (Fig. 16E, F). These results show that the selective activation of PV+ interneurons, but not SOM+ interneurons, in the ACC is able to reverse the effects of inflammation on the mechanical pain threshold, without affecting the mechanical pain threshold under basal conditions.

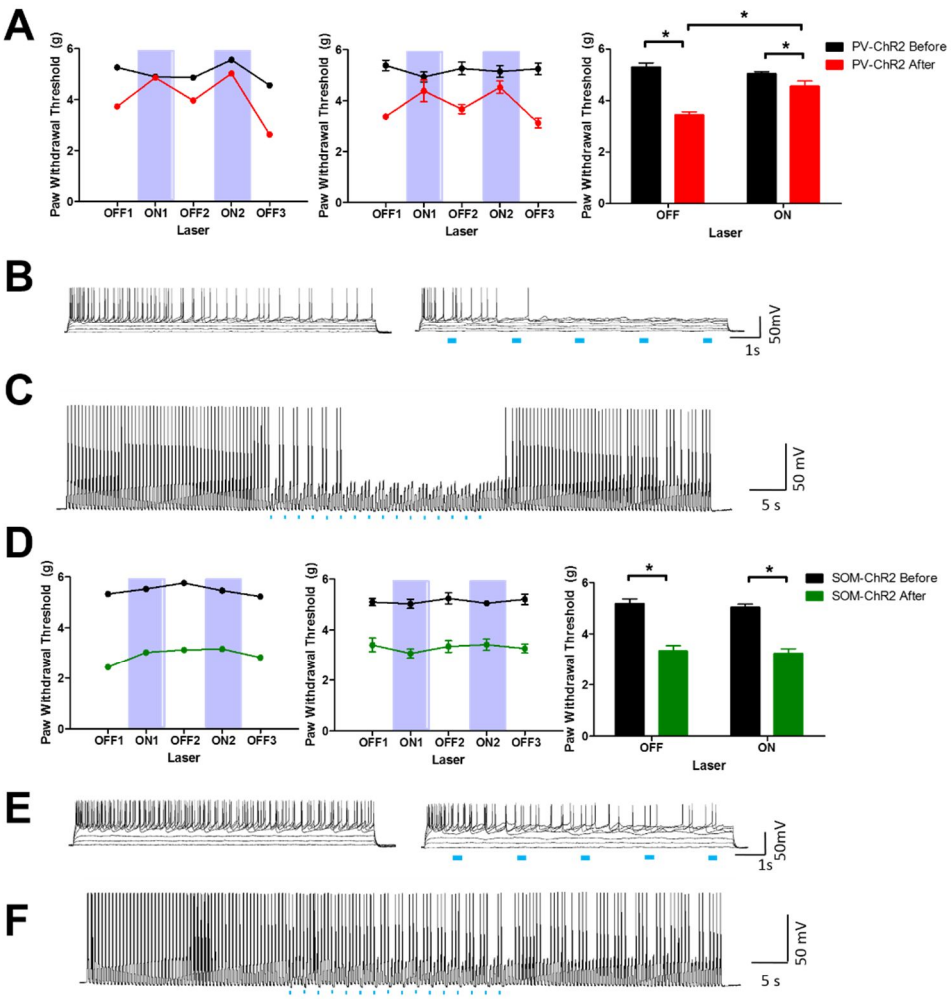
A
Paw Withdrawal Threshold (g)
OFF1 ON1 OFF2 ON2 OFF3
Laser
OFF ON
PV-ChR2 Before
PV-ChR2 After
B
50mV
1s
C
50 mV
5 s
D
SOM-ChR2 Before
SOM-ChR2 After
E
50mV
1s
F
50 mV
5 s

Figure 16. Activation of PV-positive interneurons in the ACC alleviates the CFA-induced decrease of the mechanical threshold

A, Results of the PV-ChR2 CFA group. There was no effect of blue light before (black) CFA (off: 5.30±0.15 g, on: 5.04±0.07 g; n = 6) however, there was significant effect after (red) CFA injection (off: 3.44±0.11 g, on: 4.55±0.21 g; n = 6) [p = 0.002 in CFA and laser interaction, two-way repeated measures ANOVA].

B, Result of current injection experiment with PV-ChR2 mice. A pyramidal neuron in the ACC was current clamped and current was injected without (left) and with blue light (right). Blue dots indicate illumination periods. Firing rates of the pyramidal neurons decreased when light was given.

C, Result of pulse train experiment with PV-ChR2 mice. A pyramidal neuron in the ACC was current- clamped and current pulses were given for 90 s while light was given for 30 s as indicated by the blue dots. Firing of the pyramidal neurons decreased as a result of illumination.

D, Result of the SOM-ChR2 CFA group. There was no light effect either before (off: 5.11 ± 0.15 g, on: 4.95 ± 0.11 g; n = 12) or after CFA injection (off: 3.32 ± 0.16 g, on: 3.30 ± 0.13 g; n = 12).

E, Result of current injection experiment with SOM-ChR2 mice. Light had only a small effect on the firing of pyramidal neurons.

F, Result of pulse train experiment with SOM-ChR2 mice. Light had only a small effect on firing rate.

DISCUSSION

In the present study, we have demonstrated that neurons within the ACC are acutely involved in the nociceptive responses of painful stimuli. We found that the specific activation of excitatory neurons in the ACC results in a lowering of the mechanical pain threshold, which is consistent with the view that the ACC is important in nociceptive responses (Fuchs et al., 2014; Koga et al., 2010; Vogt, 2005; Zhuo, 2008). Interestingly, the effect occurred rapidly upon optogenetic excitation, was rapidly reversible upon termination of illumination and was reproducible upon a second trial. This strongly suggests that these ACC neurons are effectors of the nociceptive responses as opposed to being a secondary reporter of the stimulus. This may be due to activating the descending facilitation projection(Chen et al., 2014a). Of course, our findings do not exclude the possibility that there are other primary mediators of the nociceptive responses. However, the observation that simply exciting a proportion of excitatory neurons in the ACC was able to significantly modify the mechanical pain threshold demonstrates the key role played by these neurons.

The observation that optogenetic excitation of excitatory ACC neurons was unable to further lower the mechanical pain threshold in mice treated with CFA suggests an occlusion between the two effects. In other words, an increase in activity in these ACC neurons may be mediating the nociceptive responses of inflammatory pain. If this is the case, the prediction would be that optogenetic inhibition of this neuronal may reverse the effects of inflammation on the mechanical pain threshold. The finding that optogenetic inhibition of excitatory

ACC neurons had a substantial effect on the mechanical threshold after CFA treatment strongly suggests that these neurons do indeed convey this nociceptive signal. Interestingly, optogenetic inhibition of these neurons had no effect under normal (non-inflammatory) conditions. Thus, an increase in activity of this neuronal population signals the hyperalgesic state. When considered together these results imply that excitatory neurons in the ACC are both necessary and sufficient to mediate sensitization to mechanical stimuli.

Excitatory neurons in the cortex are under strong regulation by GABAergic interneurons. We found that optogenetic stimulation of one class, PV-containing interneurons, was sufficient to have a substantial effect on the pain threshold. This effect was again specific for the inflamed state. Indeed, in all respects, stimulation of this single interneuron class mimicked the effects of inhibition of the excitatory neurons within this brain structure. This observation is consistent with the role of PV+ interneurons as mediators of powerful feed-forward inhibition of pyramidal neurons(Delevich et al., 2015). It shows that excitatory ACC neurons are under powerful influence of this interneuronal subclass during painful stimuli and that their specific activation is sufficient to alleviate mechanical hypersensitivity, presumably by their inhibition of pyramidal neurons in the ACC. Recently, an opposite conclusion has been reached with respect to the role of the mPFC, especially the prelimbic cortex (PL), in the processing of painful information. Activation of PL excitatory neurons reduced pain(Wang et al., 2015), and activation of PV interneurons induced more pain(Zhang et al., 2015). Moreover, activation of PL projection to nucleus accumbens relieved pain(Lee et

al., 2015). These results highlight how anatomically distinct cortical regions have discrete roles in pain processing.

Recently two other studies have used optogenetic approaches to address specifically the functional roles of the ACC but they drew different conclusions. In one study it was reported that optogenetic stimulation of Thy1-ChR2 mice did not affect the mechanical threshold (Barthas et al., 2015) whereas in the other study it was reported that activation of Thy1-ChR2 mice resulted in analgesia (Gu et al., 2015). Why the two studies reached different conclusions is unclear, though it may be due to the use of different Thy1-ChR2 mice lines. There are several possibilities why our conclusions differs from the study of Barthas et al (36). Firstly, in the Thy1 mouse there is expression of ChR2 in multiple neuronal types. Indeed, we found that specific activation of ChR2 in pyramidal neurons and PV+ interneurons had diametrically-opposed effects. Secondly, in this previous study, optogenetic stimulation and the mechanical threshold test were not performed at the same time. Therefore, this raises the possibility that chronic activation of ACC excitatory neurons does not affect the mechanical threshold but rather this requires their acute activation. Our study does, however, agree with the report of Gu et al (37), which attributed the analgesia to the activation of inhibitory neurons, and extends these findings by identifying PV+ neurons as a critical inhibitory neuronal class.

In the study by Barthas et al (2015) it was reported that optogenetic stimulation resulted in a long lasting alterations in anxiety and depressive-like behaviors (Barthas et al., 2015). In the present study we did not observe any

effects of optogenetic manipulation on anxiety-like behavior, as assessed using the open field test. This difference could be explained by the need for repeated stimulation to elicit mood-related behaviors and/or because in the Thy1-ChR2 mice mixed cell types are affected.

In conclusion, we have identified two specific neuronal types within the ACC that are involved in the nociceptive responses to inflammatory pain. These results raise the possibility that specifically targeting these neuronal populations may lead to effective treatments of painful states.

CONCLUSION

In this study, I investigated the characteristics of mice ACC in pain related situations with electrophysiology and optogenetics.

In Chapter II, I focused on ACC LTD with a multi-electrode array system. Spatial distribution of LTD showing areas can be detected with this device and could collect much more data than the conventional field recording system. I found that 1 Hz LFS was the most efficient protocol to induce LTD. This LFS-induced ACC LTD was mGluR and L-VGCC dependent and partially NMDAR dependent and this was impaired after tail amputation. Using mGluR1 priming effect, I could recover ACC LTD in tail amputated mice. This process was PKC dependent.

In Chapter III, I used optogenetics in chronic inflammation pain model to modulate acitivity of ACC neurons. Activation of ACC excitatory neurons reduced the mechanical threshold but was occluded when CFA was given. Inhibition of ACC excitatory neurons partially recovered CFA induced hyperalgesia and this phenomenon was also observed when PV-positive interneurons were activated in CFA injected mice. However, activation of SOM-positive interneurons had no effect in this behavior.

Further studies will address pile of questions about function of ACC in

pain related behaviors. There have been several in vitro studies on the molecular mechanisms of pain in the synaptic level of ACC, however not much have been investigating in the circuit level. Therefore, a systemic approach for circuit study of pain within ACC and between other brain regions would possibly be the next important investigation in this field. Optogenetics will be the best tool for this kind of study and will give a better understanding of the pain circuit.

REFERENCE

Abraham, W.C. (2008). Metaplasticity: tuning synapses and networks for plasticity. Nature reviews Neuroscience *9*, 387.

Apkarian, A.V., Bushnell, M.C., Treede, R.D., and Zubieta, J.K. (2005). Human brain mechanisms of pain perception and regulation in health and disease. Eur J Pain *9*, 463-484.

Barthas, F., Sellmeijer, J., Hugel, S., Waltisperger, E., Barrot, M., and Yalcin, I. (2015). The anterior cingulate cortex is a critical hub for pain-induced depression. Biological psychiatry *77*, 236-245.

Bashir, Z.I., Bortolotto, Z.A., Davies, C.H., Berretta, N., Irving, A.J., Seal, A.J., Henley, J.M., Jane, D.E., Watkins, J.C., and Collingridge, G.L. (1993a). Induction of LTP in the hippocampus needs synaptic activation of glutamate metabotropic receptors. Nature *363*, 347-350.

Bashir, Z.I., Jane, D.E., Sunter, D.C., Watkins, J.C., and Collingridge, G.L. (1993b). Metabotropic glutamate receptors contribute to the induction of long-term depression in the CA1 region of the hippocampus. European journal of pharmacology *239*, 265-266.

Blake, J.F., Brown, M.W., and Collingridge, G.L. (1988). CNQX blocks acidic amino acid induced depolarizations and synaptic components mediated by non-NMDA receptors in rat hippocampal slices. Neuroscience letters *89*, 182-186.

Bliss, T.V., and Cooke, S.F. (2011). Long-term potentiation and long-term depression: a clinical perspective. Clinics (Sao Paulo) *66 Suppl 1*, 3-17.

Bortolotto, Z.A., Bashir, Z.I., Davies, C.H., and Collingridge, G.L. (1994). A molecular switch activated by metabotropic glutamate receptors regulates induction of long-term potentiation. Nature *368*, 740-743.

Bortolotto, Z.A., and Collingridge, G.L. (1998). Involvement of calcium/calmodulin-dependent protein kinases in the setting of a molecular switch involved in hippocampal LTP. Neuropharmacology *37*, 535-544.

Bortolotto, Z.A., and Collingridge, G.L. (2000). A role for protein kinase C in a form of metaplasticity that regulates the induction of long-term potentiation at CA1 synapses of the adult rat hippocampus. The European journal of neuroscience *12*, 4055-4062.

Brandon, E.P., Zhuo, M., Huang, Y.Y., Qi, M., Gerhold, K.A., Burton, K.A., Kandel, E.R., McKnight, G.S., and Idzerda, R.L. (1995). Hippocampal long-term depression and depotentiation are defective in mice carrying a targeted disruption of the gene encoding the RI beta subunit of cAMP-dependent protein kinase.

Proceedings of the National Academy of Sciences of the United States of America *92*, 8851-8855.

Brebner, K., Wong, T.P., Liu, L., Liu, Y., Campsall, P., Gray, S., Phelps, L., Phillips, A.G., and Wang, Y.T. (2005). Nucleus accumbens long-term depression and the expression of behavioral sensitization. Science *310*, 1340-1343.

Bush, G., Luu, P., and Posner, M.I. (2000). Cognitive and emotional influences in anterior cingulate cortex. Trends Cogn Sci *4*, 215-222.

Calejesan, A.A., Kim, S.J., and Zhuo, M. (2000). Descending facilitatory modulation of a behavioral nociceptive response by stimulation in the adult rat anterior cingulate cortex. European journal of pain *4*, 83-96.

Casey, K.L. (1999). Forebrain mechanisms of nociception and pain: analysis through imaging. Proceedings of the National Academy of Sciences of the United States of America *96*, 7668-7674.

Chen, T., Koga, K., Descalzi, G., Qiu, S., Wang, J., Zhang, L.S., Zhang, Z.J., He, X.B., Qin, X., Xu, F.Q.*, et al.* (2014a). Postsynaptic potentiation of corticospinal projecting neurons in the anterior cingulate cortex after nerve injury. Molecular pain *10*, 33.

Chen, T., Wang, W., Dong, Y.L., Zhang, M.M., Wang, J., Koga, K., Liao, Y.H., Li, J.L., Budisantoso, T., Shigemoto, R.*, et al.* (2014b). Postsynaptic insertion of AMPA receptor onto cortical pyramidal neurons in the anterior cingulate cortex after peripheral nerve injury. Molecular brain *7*, 76.

Cohen, A.S., Raymond, C.R., and Abraham, W.C. (1998). Priming of long-term potentiation induced by activation of metabotropic glutamate receptors coupled to phospholipase C. Hippocampus *8*, 160-170.

Collingridge, G.L., Peineau, S., Howland, J.G., and Wang, Y.T. (2010). Long-term depression in the CNS. Nature reviews Neuroscience *11*, 459-473.

Conquet, F., Bashir, Z.I., Davies, C.H., Daniel, H., Ferraguti, F., Bordi, F., Franz-Bacon, K., Reggiani, A., Matarese, V., Conde, F.*, et al.* (1994). Motor deficit and impairment of synaptic plasticity in mice lacking mGluR1. Nature *372*, 237-243.

Craig, A.D., Reiman, E.M., Evans, A., and Bushnell, M.C. (1996). Functional imaging of an illusion of pain. Nature *384*, 258-260.

de Tommaso, M., Losito, L., Difruscolo, O., Libro, G., Guido, M., and Livrea, P. (2005). Changes in cortical processing of pain in chronic migraine. Headache *45*, 1208-1218.

Delevich, K., Tucciarone, J., Huang, Z.J., and Li, B. (2015). The Mediodorsal Thalamus Drives Feedforward Inhibition in the Anterior Cingulate Cortex via

Parvalbumin Interneurons. The Journal of neuroscience : the official journal of the Society for Neuroscience *35*, 5743-5753.

Dolen, G., Osterweil, E., Rao, B.S., Smith, G.B., Auerbach, B.D., Chattarji, S., and Bear, M.F. (2007). Correction of fragile X syndrome in mice. Neuron *56*, 955-962.

Dolmetsch, R.E., Pajvani, U., Fife, K., Spotts, J.M., and Greenberg, M.E. (2001). Signaling to the nucleus by an L-type calcium channel-calmodulin complex through the MAP kinase pathway. Science *294*, 333-339.

Dudek, S.M., and Bear, M.F. (1992). Homosynaptic long-term depression in area CA1 of hippocampus and effects of N-methyl-D-aspartate receptor blockade. Proceedings of the National Academy of Sciences of the United States of America *89*, 4363-4367.

Dunckley, P., Wise, R.G., Aziz, Q., Painter, D., Brooks, J., Tracey, I., and Chang, L. (2005). Cortical processing of visceral and somatic stimulation: differentiating pain intensity from unpleasantness. Neuroscience *133*, 533-542.

Eisenberger, N.I., Lieberman, M.D., and Williams, K.D. (2003). Does rejection hurt? An FMRI study of social exclusion. Science *302*, 290-292.

Fuchs, P.N., Peng, Y.B., Boyette-Davis, J.A., and Uhelski, M.L. (2014). The anterior cingulate cortex and pain processing. Frontiers in integrative neuroscience *8*, 35.

Gu, L., Uhelski, M.L., Anand, S., Romero-Ortega, M., Kim, Y.T., Fuchs, P.N., and Mohanty, S.K. (2015). Pain inhibition by optogenetic activation of specific anterior cingulate cortical neurons. PloS one *10*, e0117746.

Hayashi, Y., Shi, S.H., Esteban, J.A., Piccini, A., Poncer, J.C., and Malinow, R. (2000). Driving AMPA receptors into synapses by LTP and CaMKII: requirement for GluR1 and PDZ domain interaction. Science *287*, 2262-2267.

Hickey, L., Li, Y., Fyson, S.J., Watson, T.C., Perrins, R., Hewinson, J., Teschemacher, A.G., Furue, H., Lumb, B.M., and Pickering, A.E. (2014). Optoactivation of locus ceruleus neurons evokes bidirectional changes in thermal nociception in rats. The Journal of neuroscience : the official journal of the Society for Neuroscience *34*, 4148-4160.

Hofmann, F., and Bading, H. (2006). Long term recordings with microelectrode arrays: studies of transcription-dependent neuronal plasticity and axonal regeneration. J Physiol Paris *99*, 125-132.

Hutchison, W.D., Davis, K.D., Lozano, A.M., Tasker, R.R., and Dostrovsky, J.O. (1999). Pain-related neurons in the human cingulate cortex. Nature neuroscience *2*, 403-405.

Iwata, K., Kamo, H., Ogawa, A., Tsuboi, Y., Noma, N., Mitsuhashi, Y., Taira, M., Koshikawa, N., and Kitagawa, J. (2005). Anterior cingulate cortical neuronal activity during perception of noxious thermal stimuli in monkeys. Journal of neurophysiology *94*, 1980-1991.

Iyer, S.M., Montgomery, K.L., Towne, C., Lee, S.Y., Ramakrishnan, C., Deisseroth, K., and Delp, S.L. (2014). Virally mediated optogenetic excitation and inhibition of pain in freely moving nontransgenic mice. Nature biotechnology *32*, 274-278.

Johansen, J.P., Fields, H.L., and Manning, B.H. (2001). The affective component of pain in rodents: direct evidence for a contribution of the anterior cingulate cortex. Proceedings of the National Academy of Sciences of the United States of America *98*, 8077-8082.

Kim, J.I., Lee, H.R., Sim, S.E., Baek, J., Yu, N.K., Choi, J.H., Ko, H.G., Lee, Y.S., Park, S.W., Kwak, C.*, et al.* (2011). PI3Kgamma is required for NMDA receptor-dependent long-term depression and behavioral flexibility. Nature neuroscience *14*, 1447-1454.

Kirkwood, A., Dudek, S.M., Gold, J.T., Aizenman, C.D., and Bear, M.F. (1993). Common forms of synaptic plasticity in the hippocampus and neocortex in vitro. Science *260*, 1518-1521.

Koechlin, E., Ody, C., and Kouneiher, F. (2003). The architecture of cognitive control in the human prefrontal cortex. Science *302*, 1181-1185.

Koga, K., Li, X., Chen, T., Steenland, H.W., Descalzi, G., and Zhuo, M. (2010). In vivo whole-cell patch-clamp recording of sensory synaptic responses of cingulate pyramidal neurons to noxious mechanical stimuli in adult mice. Molecular pain *6*, 62.

Koyama, T., Kato, K., and Mikami, A. (2000). During pain-avoidance neurons activated in the macaque anterior cingulate and caudate. Neuroscience letters *283*, 17-20.

Koyama, T., Tanaka, Y.Z., and Mikami, A. (1998). Nociceptive neurons in the macaque anterior cingulate activate during anticipation of pain. Neuroreport *9*, 2663-2667.

Kuo, C.C., and Yen, C.T. (2005). Comparison of anterior cingulate and primary somatosensory neuronal responses to noxious laser-heat stimuli in conscious, behaving rats. Journal of neurophysiology *94*, 1825-1836.

LaGraize, S.C., Labuda, C.J., Rutledge, M.A., Jackson, R.L., and Fuchs, P.N. (2004). Differential effect of anterior cingulate cortex lesion on mechanical hypersensitivity and escape/avoidance behavior in an animal model of neuropathic pain. Exp Neurol *188*, 139-148.

Lee, D.E., Kim, S.J., and Zhuo, M. (1999). Comparison of behavioral responses to noxious cold and heat in mice. Brain Res *845*, 117-121.

Lee, M., Manders, T.R., Eberle, S.E., Su, C., D'Amour, J., Yang, R., Lin, H.Y., Deisseroth, K., Froemke, R.C., and Wang, J. (2015). Activation of corticostriatal circuitry relieves chronic neuropathic pain. The Journal of neuroscience : the official journal of the Society for Neuroscience *35*, 5247-5259.

Li, X.Y., Ko, H.G., Chen, T., Descalzi, G., Koga, K., Wang, H., Kim, S.S., Shang, Y., Kwak, C., Park, S.W., *et al.* (2010). Alleviating neuropathic pain hypersensitivity by inhibiting PKMzeta in the anterior cingulate cortex. Science *330*, 1400-1404.

Liauw, J., Wu, L.J., and Zhuo, M. (2005). Calcium-stimulated adenylyl cyclases required for long-term potentiation in the anterior cingulate cortex. Journal of neurophysiology *94*, 878-882.

Likhtik, E., Pelletier, J.G., Paz, R., and Pare, D. (2005). Prefrontal control of the amygdala. The Journal of neuroscience : the official journal of the Society for Neuroscience *25*, 7429-7437.

Manahan-Vaughan, D., and Braunewell, K.H. (1999). Novelty acquisition is associated with induction of hippocampal long-term depression. Proceedings of the National Academy of Sciences of the United States of America *96*, 8739-8744.

Mockett, B.G., Guevremont, D., Wutte, M., Hulme, S.R., Williams, J.M., and Abraham, W.C. (2011). Calcium/calmodulin-dependent protein kinase II mediates group I metabotropic glutamate receptor-dependent protein synthesis and long-term depression in rat hippocampus. The Journal of neuroscience : the official journal of the Society for Neuroscience *31*, 7380-7391.

Morin, F.O., Takamura, Y., and Tamiya, E. (2005). Investigating neuronal activity with planar microelectrode arrays: achievements and new perspectives. J Biosci Bioeng *100*, 131-143.

Mulkey, R.M., and Malenka, R.C. (1992). Mechanisms underlying induction of homosynaptic long-term depression in area CA1 of the hippocampus. Neuron *9*, 967-975.

Nicholls, R.E., Alarcon, J.M., Malleret, G., Carroll, R.C., Grody, M., Vronskaya, S., and Kandel, E.R. (2008). Transgenic mice lacking NMDAR-dependent LTD exhibit deficits in behavioral flexibility. Neuron *58*, 104-117.

Oh, M.C., Derkach, V.A., Guire, E.S., and Soderling, T.R. (2006). Extrasynaptic membrane trafficking regulated by GluR1 serine 845 phosphorylation primes AMPA receptors for long-term potentiation. The Journal of biological chemistry *281*, 752-758.

Oka, H., Shimono, K., Ogawa, R., Sugihara, H., and Taketani, M. (1999). A new planar multielectrode array for extracellular recording: application to hippocampal acute slice. Journal of neuroscience methods *93*, 61-67.

Oliet, S.H., Malenka, R.C., and Nicoll, R.A. (1997). Two distinct forms of long-term depression coexist in CA1 hippocampal pyramidal cells. Neuron *18*, 969-982.

Palmer, M.J., Irving, A.J., Seabrook, G.R., Jane, D.E., and Collingridge, G.L. (1997). The group I mGlu receptor agonist DHPG induces a novel form of LTD in the CA1 region of the hippocampus. Neuropharmacology *36*, 1517-1532.

Peyron, R., Laurent, B., and Garcia-Larrea, L. (2000). Functional imaging of brain responses to pain. A review and meta-analysis (2000). Neurophysiologie clinique = Clinical neurophysiology *30*, 263-288.

Pillay, P.K., and Hassenbusch, S.J. (1992). Bilateral MRI-guided stereotactic cingulotomy for intractable pain. Stereotactic and functional neurosurgery *59*, 33-38.

Qi, M., Zhuo, M., Skalhegg, B.S., Brandon, E.P., Kandel, E.R., McKnight, G.S., and Idzerda, R.L. (1996). Impaired hippocampal plasticity in mice lacking the Cbeta1 catalytic subunit of cAMP-dependent protein kinase. Proceedings of the National Academy of Sciences of the United States of America *93*, 1571-1576.

Rae, M.G., Martin, D.J., Collingridge, G.L., and Irving, A.J. (2000). Role of Ca2+ stores in metabotropic L-glutamate receptor-mediated supralinear Ca2+ signaling in rat hippocampal neurons. The Journal of neuroscience : the official journal of the Society for Neuroscience *20*, 8628-8636.

Rainville, P., Bushnell, M.C., and Duncan, G.H. (2001). Representation of acute and persistent pain in the human CNS: potential implications for chemical intolerance. Ann N Y Acad Sci *933*, 130-141.

Rainville, P., Duncan, G.H., Price, D.D., Carrier, B., and Bushnell, M.C. (1997). Pain affect encoded in human anterior cingulate but not somatosensory cortex. Science *277*, 968-971.

Sajikumar, S., and Korte, M. (2011). Metaplasticity governs compartmentalization of synaptic tagging and capture through brain-derived neurotrophic factor (BDNF) and protein kinase Mzeta (PKMzeta). Proceedings of the National Academy of Sciences of the United States of America *108*, 2551-2556.

Shyu, B.C., Chen, W.F., and Shih, H.C. (2008). Electrically and mechanically evoked nociceptive neuronal responses in the rat anterior cingulate cortex. Acta neurochirurgica Supplement *101*, 23-25.

Shyu, B.C., and Vogt, B.A. (2009). Short-term synaptic plasticity in the nociceptive thalamic-anterior cingulate pathway. Molecular pain *5*, 51.

Sikes, R.W., and Vogt, B.A. (1992). Nociceptive neurons in area 24 of rabbit cingulate cortex. Journal of neurophysiology *68*, 1720-1732.

Singer, T., Seymour, B., O'Doherty, J., Kaube, H., Dolan, R.J., and Frith, C.D. (2004). Empathy for pain involves the affective but not sensory components of pain. Science *303*, 1157-1162.

Strigo, I.A., Duncan, G.H., Boivin, M., and Bushnell, M.C. (2003). Differentiation of visceral and cutaneous pain in the human brain. Journal of neurophysiology *89*, 3294-3303.

Talbot, J.D., Marrett, S., Evans, A.C., Meyer, E., Bushnell, M.C., and Duncan, G.H. (1991). Multiple representations of pain in human cerebral cortex. Science *251*, 1355-1358.

Toyoda, H., Wu, L.J., Zhao, M.G., Xu, H., Jia, Z., and Zhuo, M. (2007a). Long-term depression requires postsynaptic AMPA GluR2 receptor in adult mouse cingulate cortex. J Cell Physiol *211*, 336-343.

Toyoda, H., Wu, L.J., Zhao, M.G., Xu, H., and Zhuo, M. (2007b). Time-dependent postsynaptic AMPA GluR1 receptor recruitment in the cingulate synaptic potentiation. Dev Neurobiol *67*, 498-509.

Toyoda, H., Zhao, M.G., and Zhuo, M. (2005). Roles of NMDA receptor NR2A and NR2B subtypes for long-term depression in the anterior cingulate cortex. Eur J Neurosci *22*, 485-494.

Tye, K.M., and Deisseroth, K. (2012). Optogenetic investigation of neural circuits underlying brain disease in animal models. Nature reviews Neuroscience *13*, 251-266.

Van den Oever, M.C., Rotaru, D.C., Heinsbroek, J.A., Gouwenberg, Y., Deisseroth, K., Stuber, G.D., Mansvelder, H.D., and Smit, A.B. (2013). Ventromedial prefrontal cortex pyramidal cells have a temporal dynamic role in recall and extinction of cocaine-associated memory. The Journal of neuroscience : the official journal of the Society for Neuroscience *33*, 18225-18233.

Vogt, B.A. (2005). Pain and emotion interactions in subregions of the cingulate gyrus. Nature reviews Neuroscience *6*, 533-544.

Wang, C.C., and Shyu, B.C. (2004). Differential projections from the mediodorsal and centrolateral thalamic nuclei to the frontal cortex in rats. Brain Res *995*, 226-235.

Wang, G.Q., Cen, C., Li, C., Cao, S., Wang, N., Zhou, Z., Liu, X.M., Xu, Y., Tian, N.X., Zhang, Y.*, et al.* (2015). Deactivation of excitatory neurons in the prelimbic cortex via Cdk5 promotes pain sensation and anxiety. Nature communications *6*,

7660.

Wang, H., Xu, H., Wu, L.J., Kim, S.S., Chen, T., Koga, K., Descalzi, G., Gong, B., Vadakkan, K.I., Zhang, X., *et al.* (2011). Identification of an adenylyl cyclase inhibitor for treating neuropathic and inflammatory pain. Science translational medicine *3*, 65ra63.

Wei, F., Li, P., and Zhuo, M. (1999). Loss of synaptic depression in mammalian anterior cingulate cortex after amputation. The Journal of neuroscience : the official journal of the Society for Neuroscience *19*, 9346-9354.

Wei, F., Qiu, C.S., Kim, S.J., Muglia, L., Maas, J.W., Pineda, V.V., Xu, H.M., Chen, Z.F., Storm, D.R., Muglia, L.J., *et al.* (2002). Genetic elimination of behavioral sensitization in mice lacking calmodulin-stimulated adenylyl cyclases. Neuron *36*, 713-726.

Wei, F., and Zhuo, M. (2001). Potentiation of sensory responses in the anterior cingulate cortex following digit amputation in the anaesthetised rat. The Journal of physiology *532*, 823-833.

West, A.E., Chen, W.G., Dalva, M.B., Dolmetsch, R.E., Kornhauser, J.M., Shaywitz, A.J., Takasu, M.A., Tao, X., and Greenberg, M.E. (2001). Calcium regulation of neuronal gene expression. Proceedings of the National Academy of Sciences of the United States of America *98*, 11024-11031.

Wolff, S.B., Grundemann, J., Tovote, P., Krabbe, S., Jacobson, G.A., Muller, C., Herry, C., Ehrlich, I., Friedrich, R.W., Letzkus, J.J., *et al.* (2014). Amygdala interneuron subtypes control fear learning through disinhibition. Nature *509*, 453-458.

Wong, E.T., Gunes, S., Gaughan, E., Patt, R.B., Ginsberg, L.E., Hassenbusch, S.J., and Payne, R. (1997). Palliation of intractable cancer pain by MRI-guided cingulotomy. The Clinical journal of pain *13*, 260-263.

Wu, J., Rowan, M.J., and Anwyl, R. (2004). Synaptically stimulated induction of group I metabotropic glutamate receptor-dependent long-term depression and depotentiation is inhibited by prior activation of metabotropic glutamate receptors and protein kinase C. Neuroscience *123*, 507-514.

Wu, L.J., Li, X., Chen, T., Ren, M., and Zhuo, M. (2009). Characterization of intracortical synaptic connections in the mouse anterior cingulate cortex using dual patch clamp recording. Molecular brain *2*, 32.

Wu, L.J., Toyoda, H., Zhao, M.G., Lee, Y.S., Tang, J., Ko, S.W., Jia, Y.H., Shum, F.W., Zerbinatti, C.V., Bu, G., *et al.* (2005a). Upregulation of forebrain NMDA NR2B receptors contributes to behavioral sensitization after inflammation. The Journal of neuroscience : the official journal of the Society for Neuroscience *25*, 11107-11116.

Wu, L.J., Xu, H., Ren, M., and Zhuo, M. (2007). Genetic and pharmacological studies of GluR5 modulation of inhibitory synaptic transmission in the anterior cingulate cortex of adult mice. Dev Neurobiol *67*, 146-157.

Wu, L.J., Zhao, M.G., Toyoda, H., Ko, S.W., and Zhuo, M. (2005b). Kainate receptor-mediated synaptic transmission in the adult anterior cingulate cortex. Journal of neurophysiology *94*, 1805-1813.

Wu, M.F., Pang, Z.P., Zhuo, M., and Xu, Z.C. (2005c). Prolonged membrane potential depolarization in cingulate pyramidal cells after digit amputation in adult rats. Molecular pain *1*, 23.

Xu, H., Wu, L.J., Wang, H., Zhang, X., Vadakkan, K.I., Kim, S.S., Steenland, H.W., and Zhuo, M. (2008). Presynaptic and postsynaptic amplifications of neuropathic pain in the anterior cingulate cortex. The Journal of neuroscience : the official journal of the Society for Neuroscience *28*, 7445-7453.

Yamamura, H., Iwata, K., Tsuboi, Y., Toda, K., Kitajima, K., Shimizu, N., Nomura, H., Hibiya, J., Fujita, S., and Sumino, R. (1996). Morphological and electrophysiological properties of ACCx nociceptive neurons in rats. Brain Res *735*, 83-92.

Yen, C.P., Kuan, C.Y., Sheehan, J., Kung, S.S., Wang, C.C., Liu, C.K., and Kwan, A.L. (2009). Impact of bilateral anterior cingulotomy on neurocognitive function in patients with intractable pain. Journal of clinical neuroscience : official journal of the Neurosurgical Society of Australasia *16*, 214-219.

Yen, C.P., Kung, S.S., Su, Y.F., Lin, W.C., Howng, S.L., and Kwan, A.L. (2005). Stereotactic bilateral anterior cingulotomy for intractable pain. Journal of clinical neuroscience : official journal of the Neurosurgical Society of Australasia *12*, 886-890.

Yizhar, O., Fenno, L.E., Davidson, T.J., Mogri, M., and Deisseroth, K. (2011). Optogenetics in neural systems. Neuron *71*, 9-34.

Zhang, Z., Gadotti, V.M., Chen, L., Souza, I.A., Stemkowski, P.L., and Zamponi, G.W. (2015). Role of Prelimbic GABAergic Circuits in Sensory and Emotional Aspects of Neuropathic Pain. Cell reports *12*, 752-759.

Zhao, M.G., Toyoda, H., Lee, Y.S., Wu, L.J., Ko, S.W., Zhang, X.H., Jia, Y., Shum, F., Xu, H., Li, B.M.*, et al.* (2005). Roles of NMDA NR2B subtype receptor in prefrontal long-term potentiation and contextual fear memory. Neuron *47*, 859-872.

Zhuo, M. (2005). Canadian Association of Neuroscience review: Cellular and synaptic insights into physiological and pathological pain. EJLB-CIHR Michael Smith Chair in Neurosciences and Mental Health lecture. Can J Neurol Sci *32*, 27-36.

Zhuo, M. (2006). Molecular mechanisms of pain in the anterior cingulate cortex. Journal of neuroscience research *84*, 927-933.

Zhuo, M. (2008). Cortical excitation and chronic pain. Trends in neurosciences *31*, 199-207.

Zhuo, M. (2011). Cortical plasticity as a new endpoint measurement for chronic pain. Molecular pain *7*, 54.

국문초록

전대상피질의 신경세포들은 통증 신호 인지와 그와 동반된 감정적 반응들에 중요한 역할을 하고 있다고 여겨지고 있다. 다양한 기술을 이용하여 전대상피질의 기능을 알아본 연구들이 많지만 아직까지 밝혀지지 않은 점들이 많이있다. 시냅스 가소성의 모델 중 하나인 장기저하는 여러 뇌 부위에서 밝혀지고 학습과 기억에 중요한 역할을 한다고 알려져 있다. 전대상피질에서도 장기저하를 유도할 수 있으며 몇가지 주요 특징들을 알아냈지만 아직 연구해야할 부분들은 많다. 따라서, 이번 연구를 통해 다중전극 시스템을 이용하여 전대상피질내의 장기저하에 대한 연구를 진행하였다. 이 영역에서의 장기저하는 mGluR, L-type 전압개폐성 칼슘채널 의존적이며 NMDAR 도 일부 중요함을 보였다. 그리고, 전대상피질 내에서 2차원적으로 장기저하가 많이 일어나는 영역들을 알아보았다. 또한, 꼬리가 절단된 쥐에서는 장기저하가 일어나지 않았다. 이를 회복시키기 위해 약하게 mGluR1을 자극시키면서 시냅스 가소성을 더 쉽게 유도할 수 있는 메타가소성을 이용해본 결과, 장기저하를 다시 유도할 수 있었고 이 과정은 PKC 의존적이라는 것도 밝혔다.

그 외에도, 전대상피질내의 다양한 종류의 신경세포들이 기능적으로 어떻게 다른지에 대한 연구는 아직 부족한 상황이다. 따라서,

그에 대한 연구를 진행하기 위해 광유전학을 이용해 보기로 하였다. 이 기술을 통해 살아있는 쥐 발에 만성염증 유도 물질인 CFA를 주었을 때와 안주었을 때에 각각 빛으로 전대상피질 신경세포들을 인위적으로 자극 또는 억제시켰을 때 통각 인지 역치값이 어떻게 변하는지 확인해 보았다. 그 결과, 흥분성 신경세포를 자극시켰을 때는 CFA 넣기 전에는 통각 인지 역치값을 낮춰 통증을 더 느끼는 것 같은 반응을 유도하였다. 그러나 CFA를 넣은 후에는 약물에 의해 낮춰진 역치값에서 더 변화를 주지는 못했다. 그리고 CFA를 넣은 후에 흥분성 신경세포를 억제시켰을 때는 CFA를 넣었을 때보다 높은 역치값을 보여서, 일부 통증을 줄인 것 같은 반응을 보였다. PV 억제성 신경세포를 자극시켰을 때도 흥분성 신경세포를 억제시켰을 때와 같은 결과가 나왔다. 하지만 SOM 억제성 신경세포에서는 아무런 변화를 관찰하지 못했다. 따라서, 전대상피질의 흥분성 신경세포가 통각인지에 주요한 역할을 하며 PV 억제성 신경세포가 이를 조절하는 역할을 한다는 것을 확인할 수 있었다는 데에 위 연구에 의의가 있다.

.....

주요어 : 전대상피질, 통증, 광유전학

학번 : 2010-22724